

Galaktikus archeológia

Kiss László, MTA CSFK CSI

Bevezetés a csillagászatba 4.



Miről lesz szó?

- A nagy vöröseltolódású Univerzum a közelben
- A Tejútrendszer szerkezete
- Égboltfelmérő programok: képek, színek, színeképek, távolságok
- Módszerek a múlt rekonstruálására

EVIDENCE FROM THE MOTIONS OF OLD STARS THAT THE GALAXY COLLAPSED

O. J. EGGEN, D. LYNDEN-BELL,* AND A. R. SANDAGE

Mount Wilson and Palomar Observatories

Carnegie Institution of Washington, California Institute of Technology

Received May 17, 1962

ABSTRACT

The (U, V, W) -velocity vectors for 221 well-observed dwarf stars have been used to compute the eccentricities and angular momenta of the galactic orbits in a model galaxy. It is shown that the eccentricity and the observed ultraviolet excess are strongly correlated. The stars with the largest excess (i.e., lowest metal abundance) are invariably moving in highly elliptical orbits, whereas stars with little or no excess move in nearly circular orbits. Correlations also exist between the ultraviolet excess and the W -velocity. Finally, the excess and the angular momentum are correlated; stars with large ultraviolet excesses have small angular momenta.

These correlations are discussed in terms of the dynamics of a collapsing galaxy. The data require that the oldest stars were formed out of gas falling toward the galactic center in the radial direction and collapsing from the halo onto the plane. The collapse was very rapid and only a few times 10^8 years were required for the gas to attain circular orbits in equilibrium (i.e., gravitational attraction balanced by centrifugal acceleration). The scale of the collapse is tentatively estimated to be at least 10 in the radial direction and 25 in the Z -direction. The initial contraction must have begun near the time of formation of the first stars, some 10^{10} years ago.

I. INTRODUCTION

Beginning with Strömberg's early investigations of stellar motions, it has become

Stars with nearly circular orbits have velocities that differ little from that of the “local standard of rest.” Although radial-velocity determinations have been made for all stars to visual magnitude 5.5, observations of fainter stars, with the exception of a few special classes of high-luminosity objects, have usually been confined to those with appreciable ($>0''.1/\text{yr}$) proper motion. This means that there is some bias in our observational data

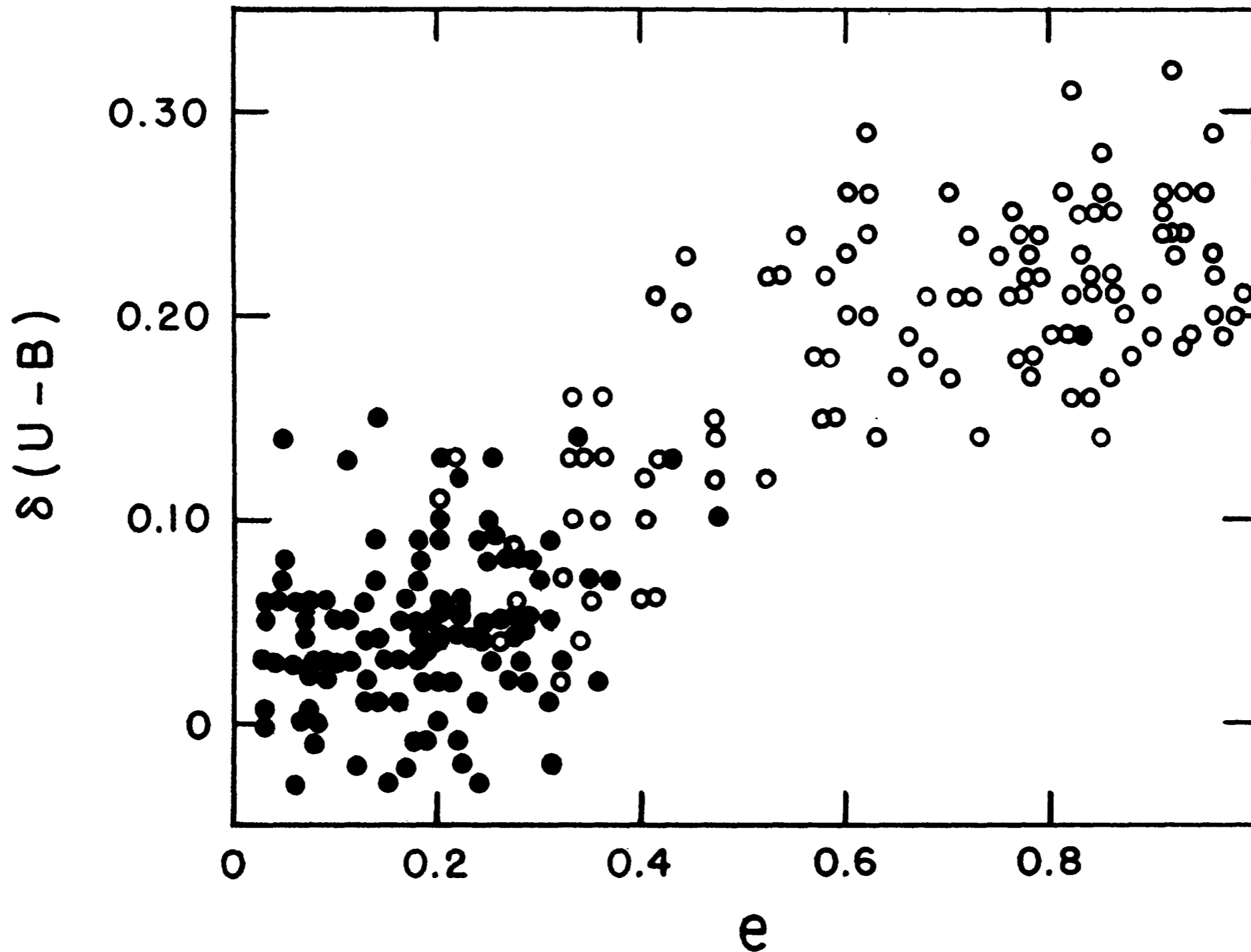


FIG. 4.—The correlation between the ultraviolet excess, $\delta(U - B)$, and the orbital eccentricity, e , for our sample of 221 stars. The filled and open circles represent stars from our first and second catalogues, respectively.

V. INTERPRETATION

If the ultraviolet excess is, in general, correlated with the ages of the stars, then *Figure 5* suggests that the oldest objects were formed at almost any height above the galactic plane,

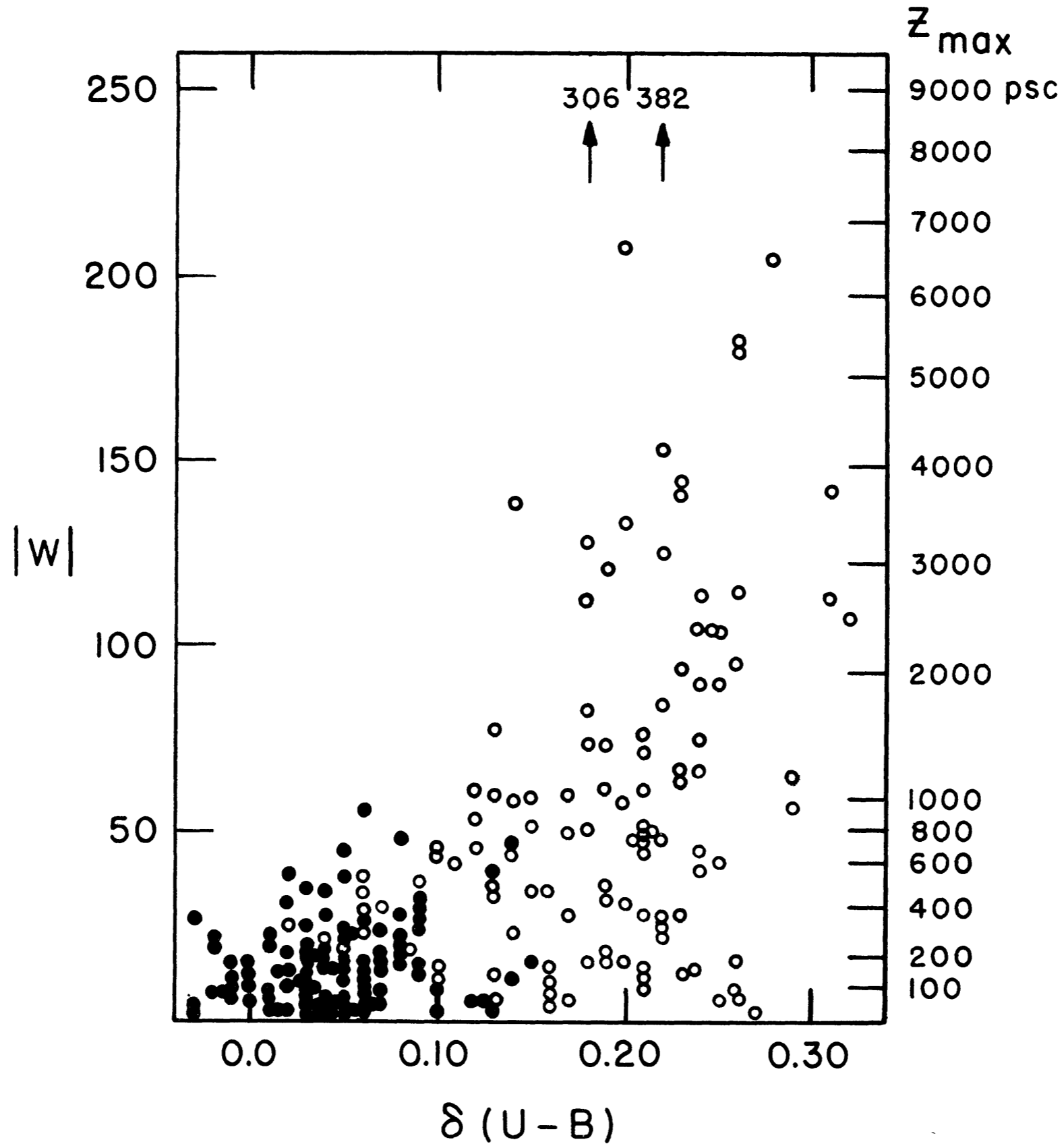
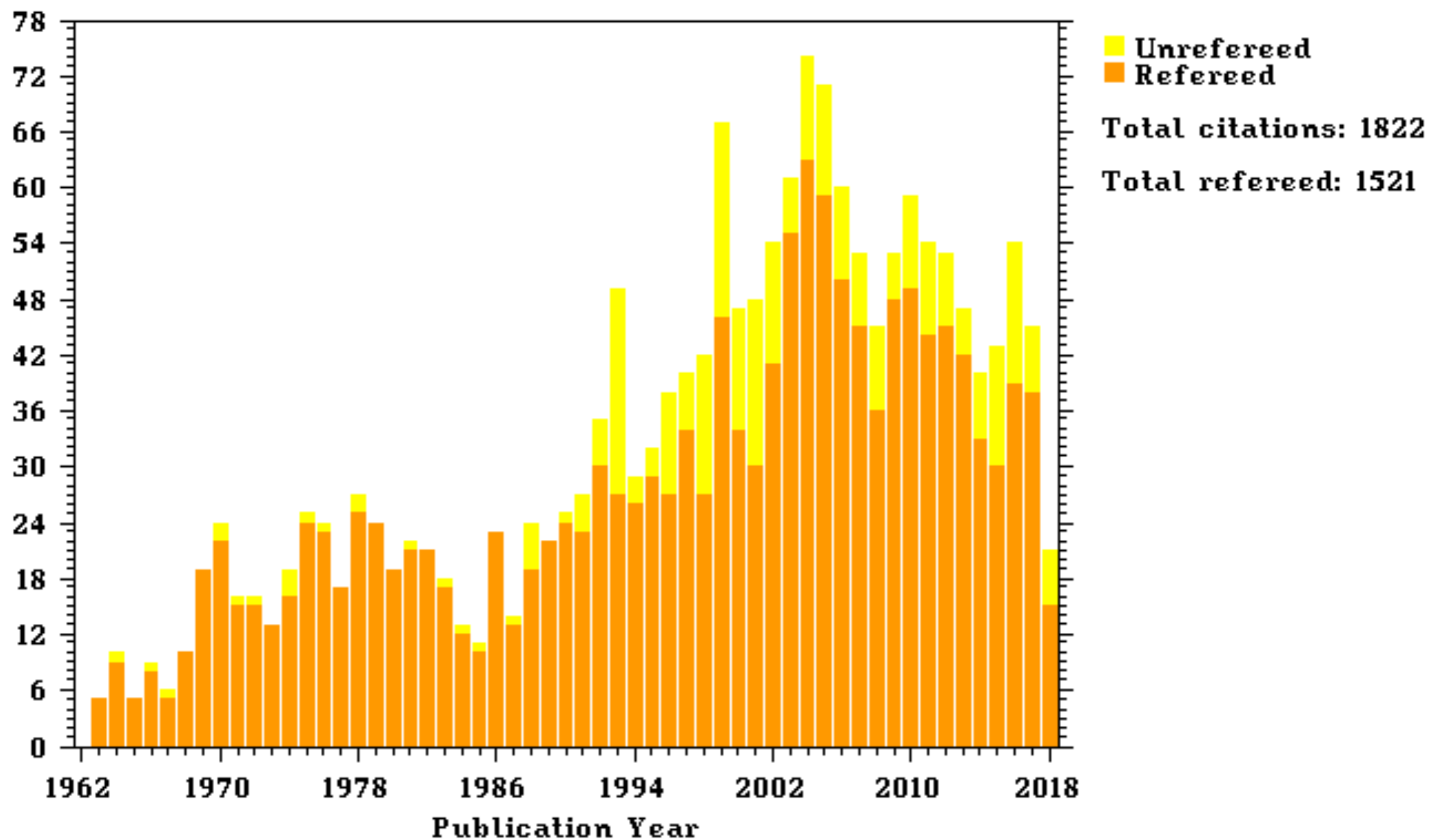


FIG 5 —The correlation between the W -velocity, perpendicular to the galactic plane, and the ultraviolet excess for the 221 stars in our sample. The filled and open circles represent the stars in our first and second catalogues, respectively.

Citations/Publication Year for 1962ApJ...136..748E



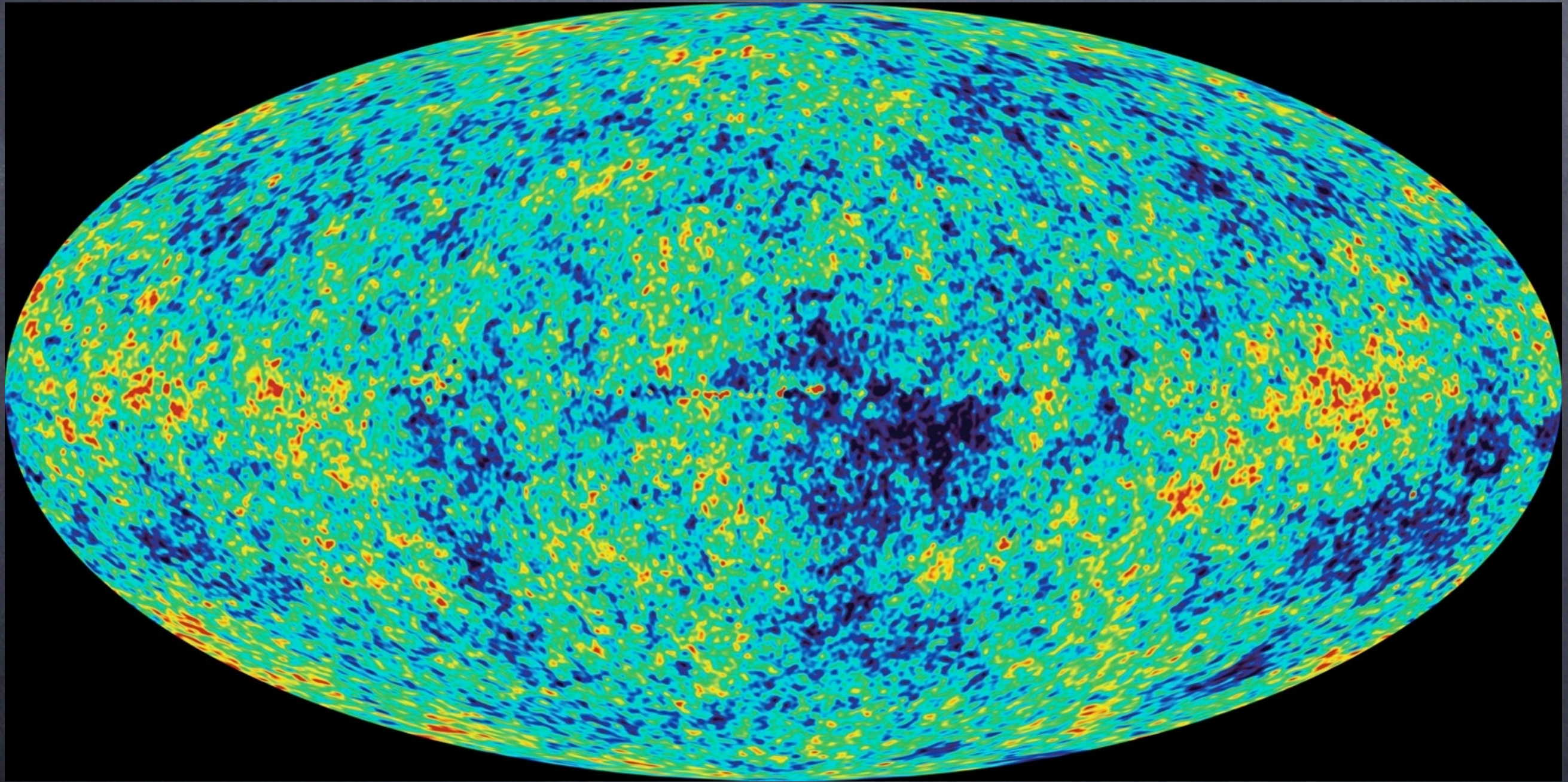
Chapter 1

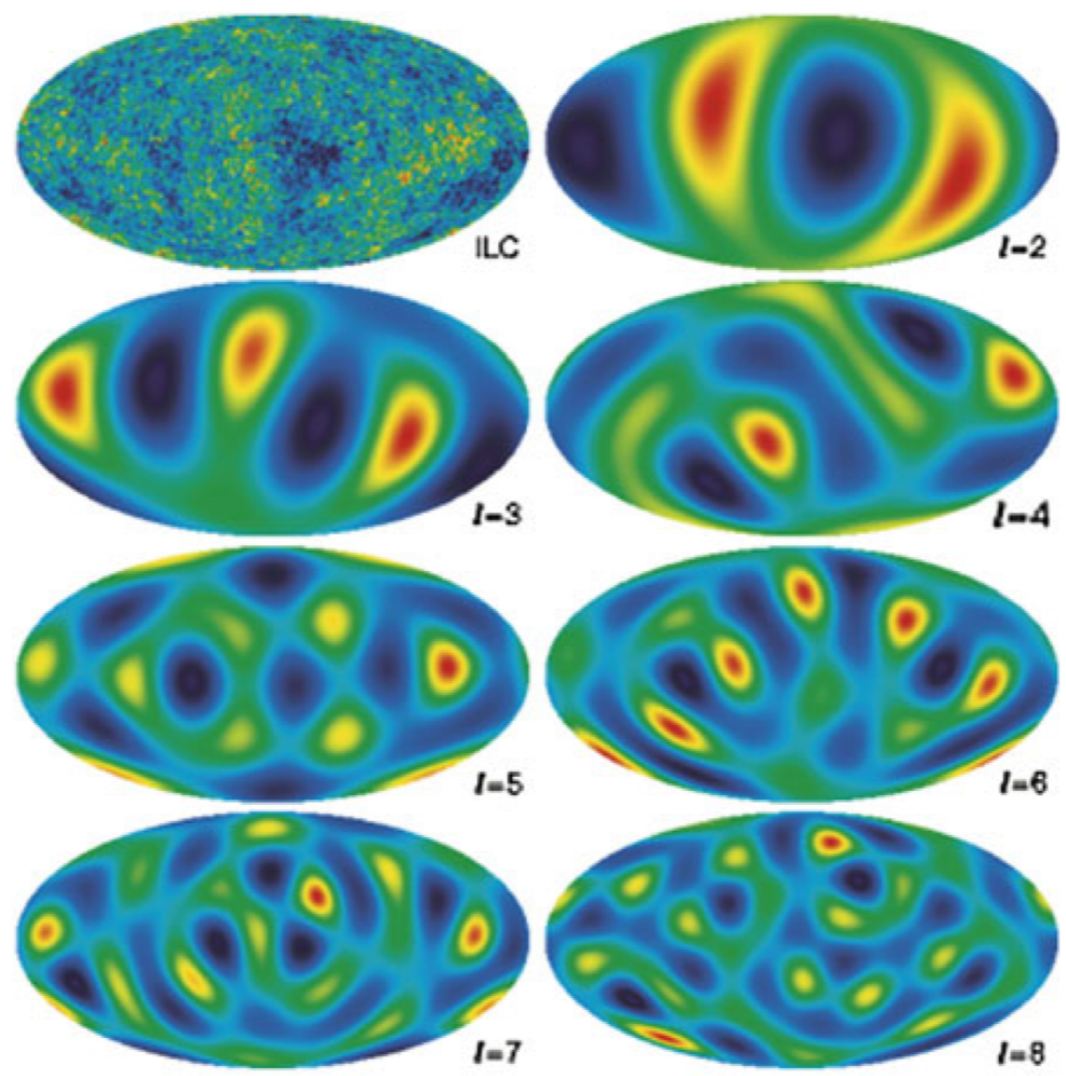
Near Field Cosmology: The Origin of the Galaxy and the Local Group

Joss Bland-Hawthorn and Kenneth Freeman

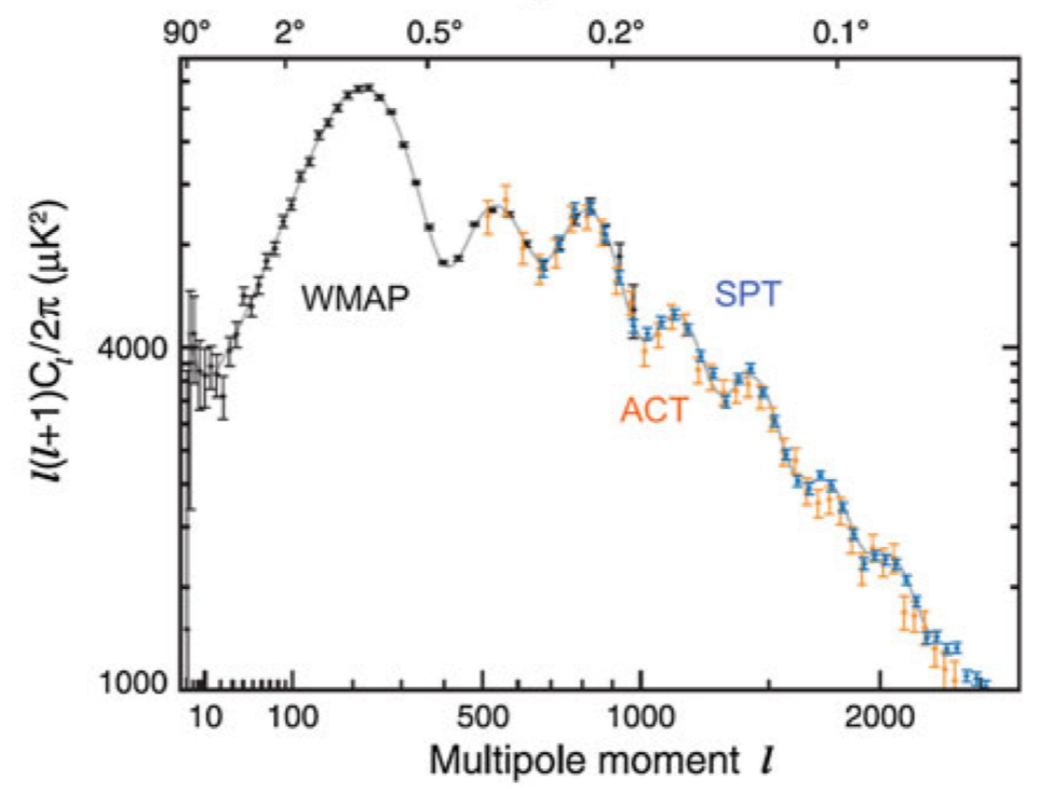
The Galaxy has built up through a process of accretion and merging over billions of years which continues to this day. Astronomers are now embarking on a new era of massive stellar surveys over the coming decade. These campaigns will derive three-dimensional space motions and heavy element abundances for millions of stars throughout the Galaxy and its neighbours. The new observations will reveal signatures of the formation and early evolution of the Local Group; this is what we mean by ‘near field cosmology.’ We set this new course of study within the context of fossil signatures from galaxy surveys and the high redshift universe. We discuss the complex relationship between baryons and dark matter over cosmic time, and introduce a synthetic framework that will allow both numerical simulations and the impending data deluge to be compared. We also include relevant source materials for the young near-field cosmologist and some historical perspectives.

A WMAP térképe a mikrohullámú
háttérsugárzásról: csomósodás **irány** szerint





Angular scale



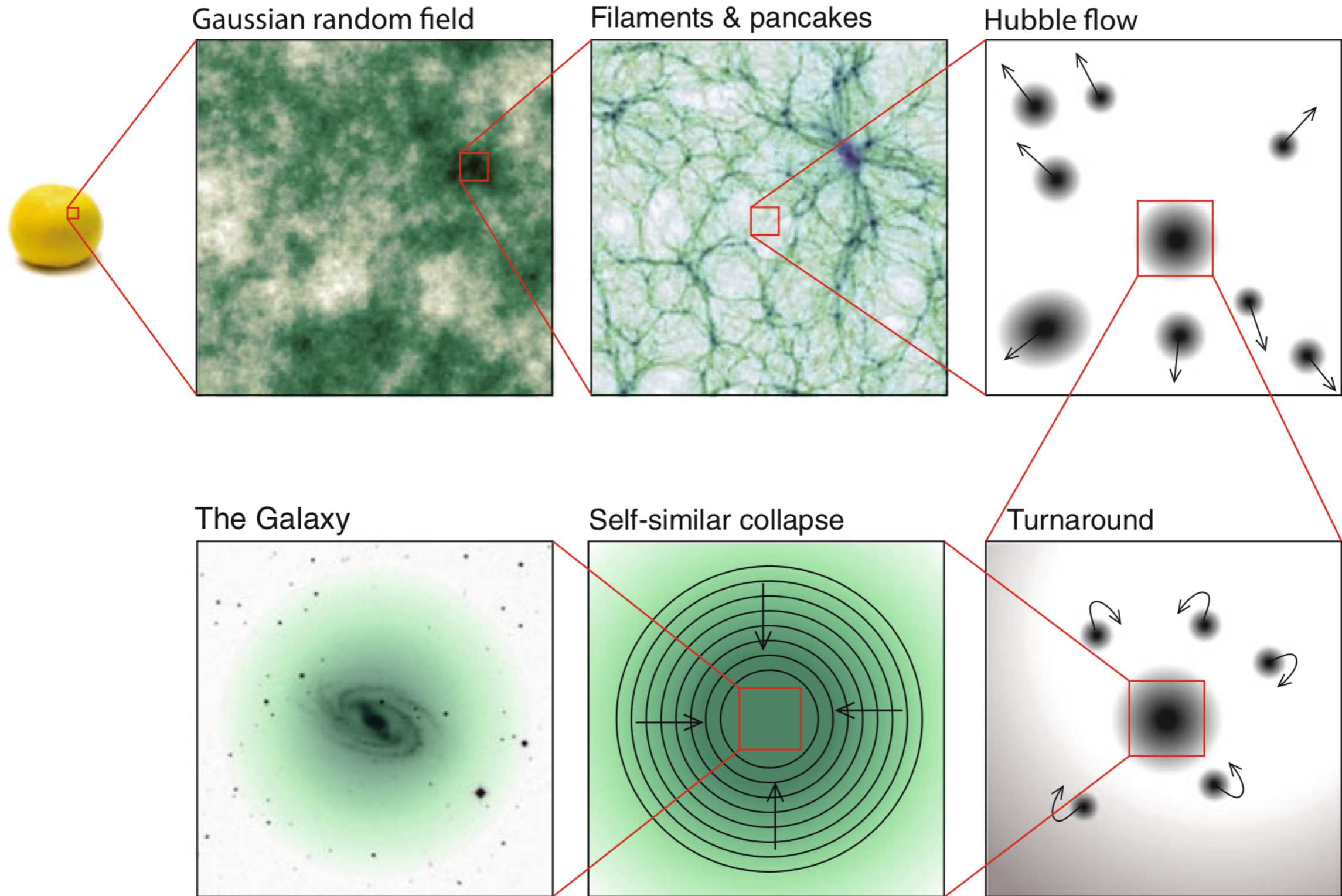


Fig. 1.15 A sequence of images depicting the major stages in the evolution of the Galaxy from the initial fluctuation spectrum—see text. This was preceded by inflation when the Universe went from sub-atomic scales to the size of a grapefruit in less than a picosecond

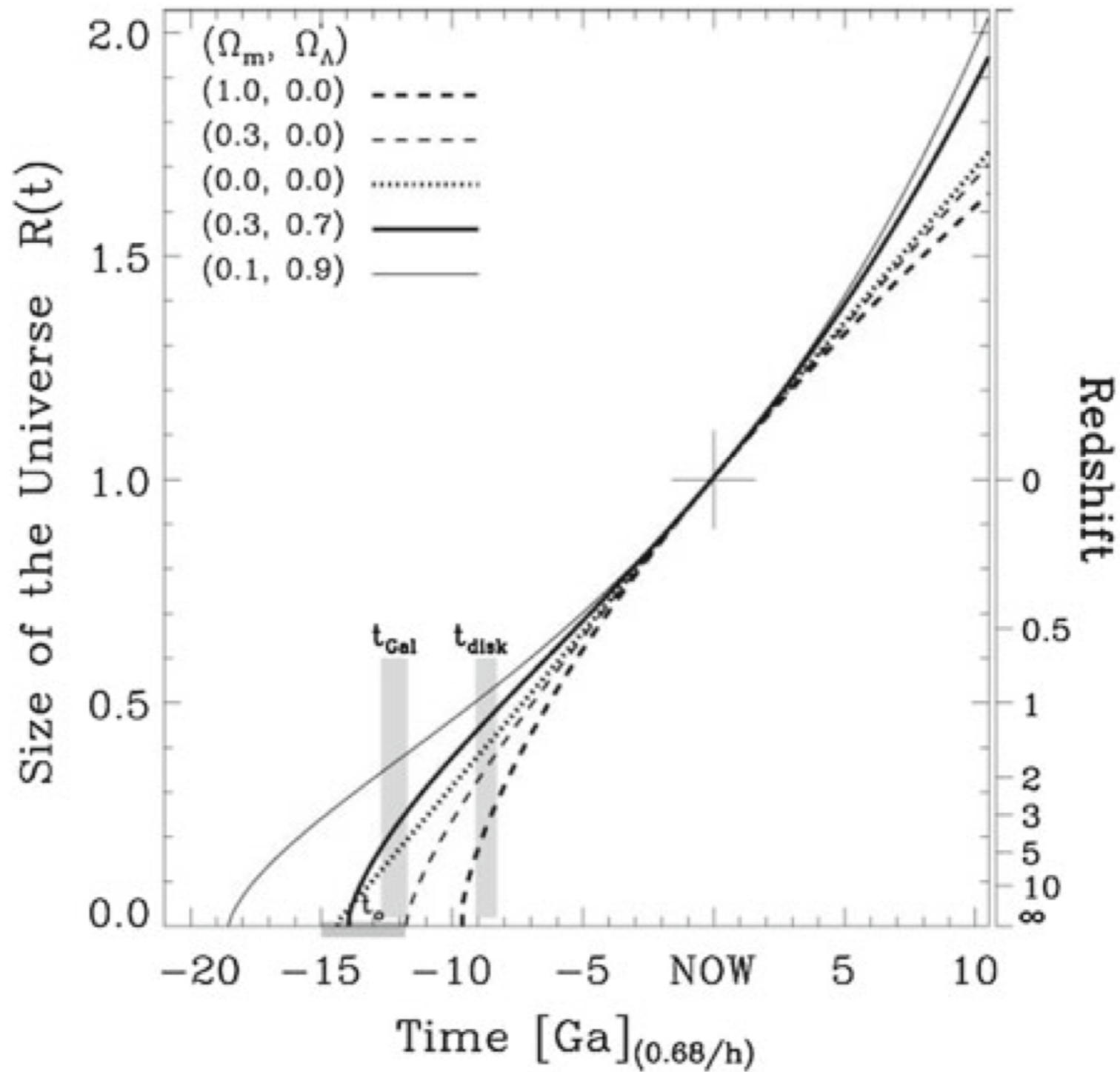


Fig. 1.14 Look-back time as a function of redshift and the size of the Universe for five different world models. The approximate ages of the Galactic halo and disk are indicated by hatched regions (we thank C. Lineweaver for modifying an earlier version of this figure for us)

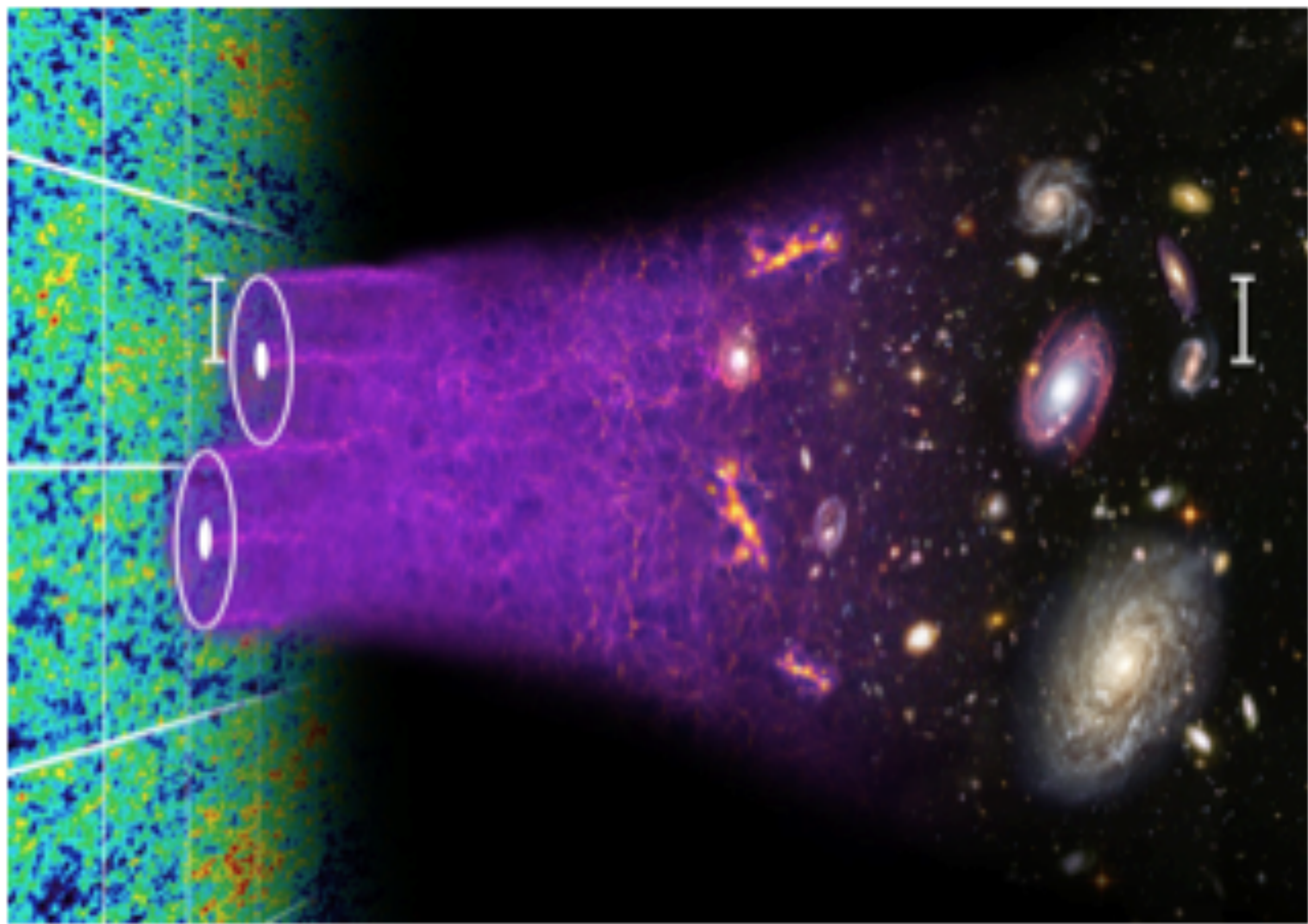
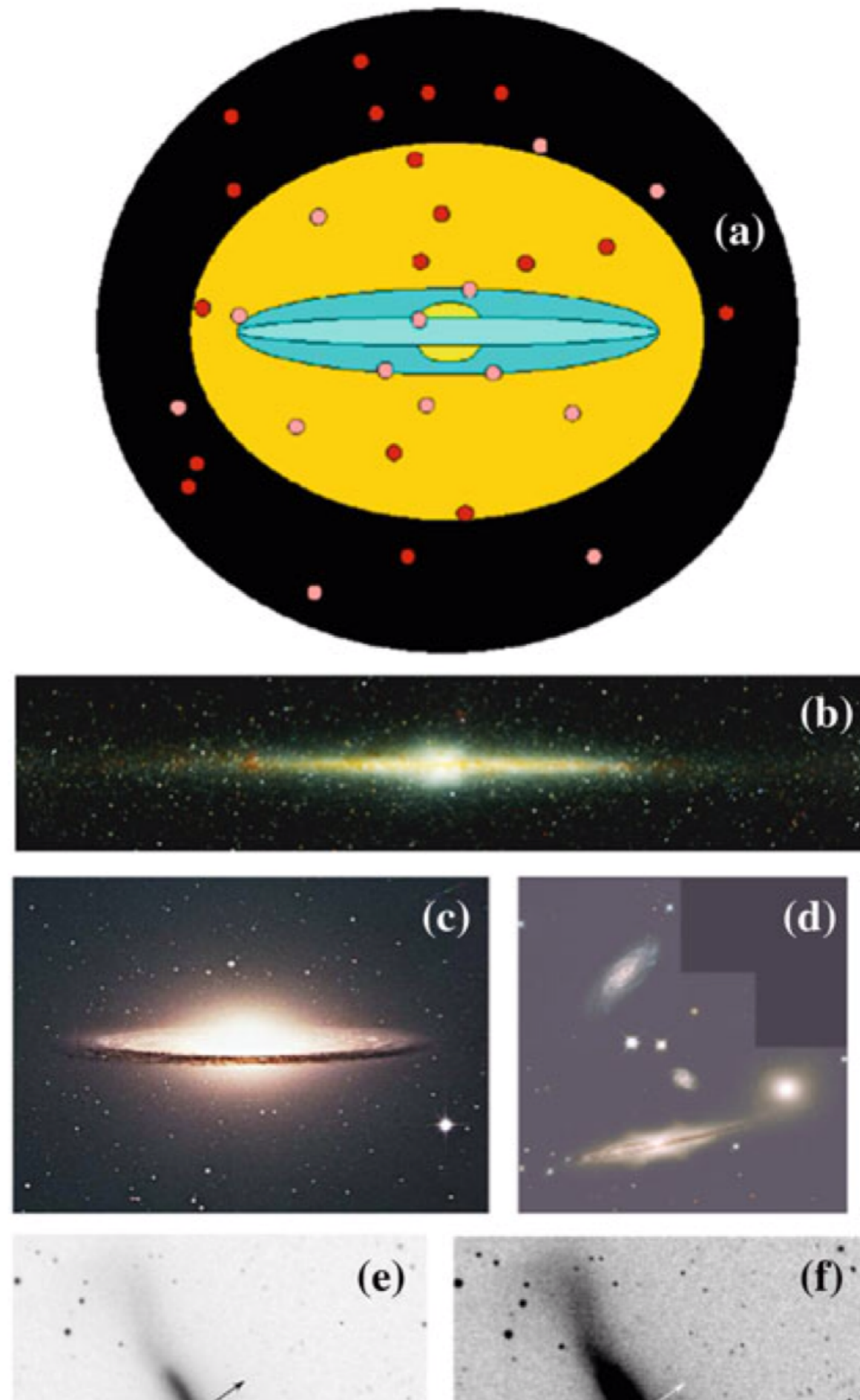


Fig. 1.19 **a** Sketch of Milky Way showing the stellar disk (*light blue*), thick disk (*dark blue*), stellar bulge (*yellow*), stellar halo (*mustard yellow*), dark halo (*black*) and globular cluster system (*filled circles*). The radius of the stellar disk is roughly 15 kpc. The baryon and dark halos extend to a radius of at least 100 kpc. **b** Infrared image of the Milky Way taken by the DIRBE instrument on board the Cosmic Background Explorer (COBE) Satellite (we acknowledge the NASA Goddard Space Flight Center and the COBE Science Working Group for this image). **c** M104, a normal disk galaxy with a large stellar bulge (from AAO). **d** Hubble Heritage image of the compact group Hickson 87; one galaxy has a peanut-shaped stellar bulge due to dynamical interaction with other group members. **e** Image of the SO galaxy NGC 4762 (Digital Sky Survey) shows its thin disk and stellar bulge. **f** A deeper image of NGC 4762 (DSS) shows



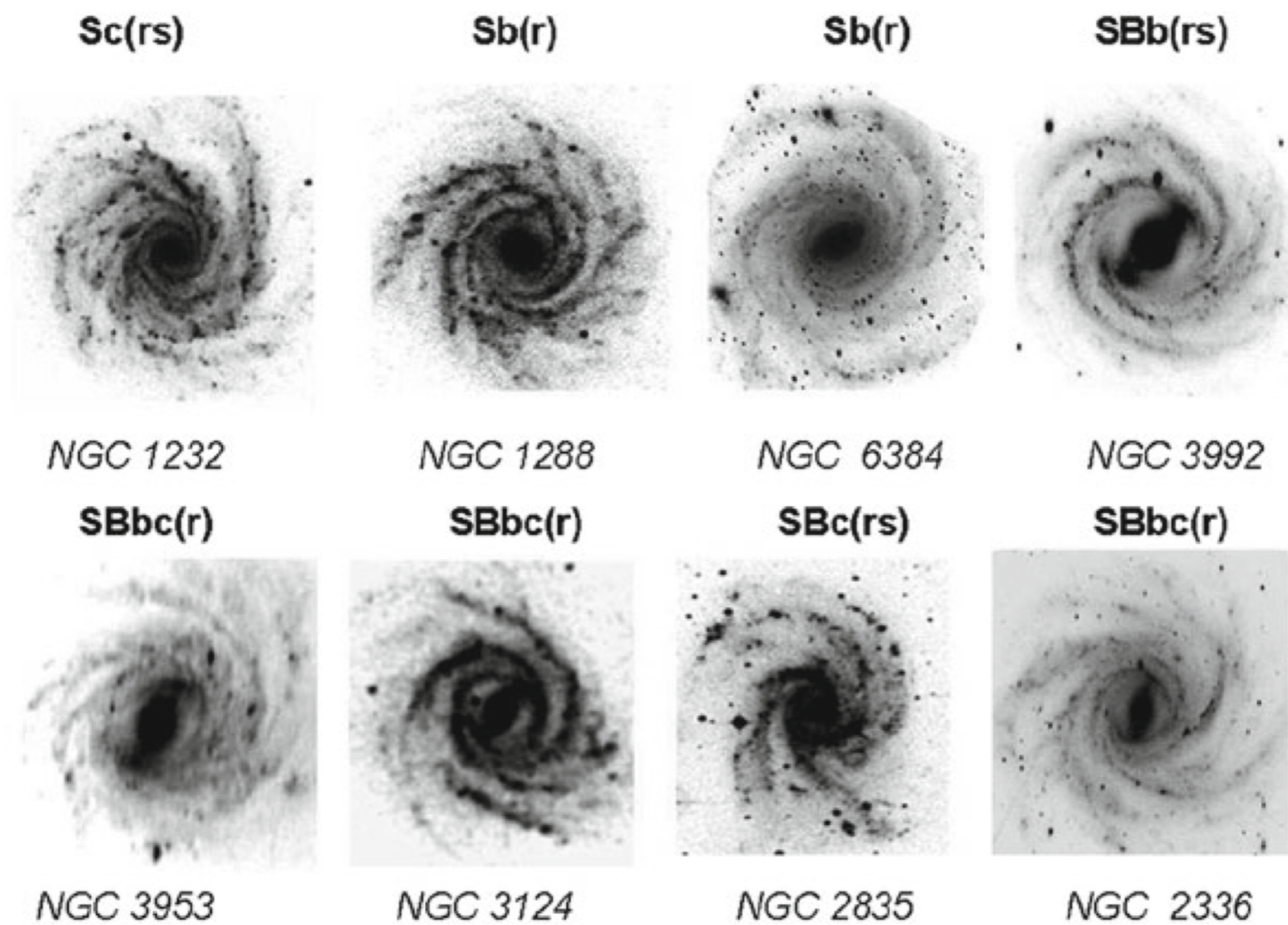


Fig. 1.18 A selection of galaxies that bear resemblance to the Milky Way (Efremov [2011](#)); NGC 3992 is arguably the closest match to the Galaxy

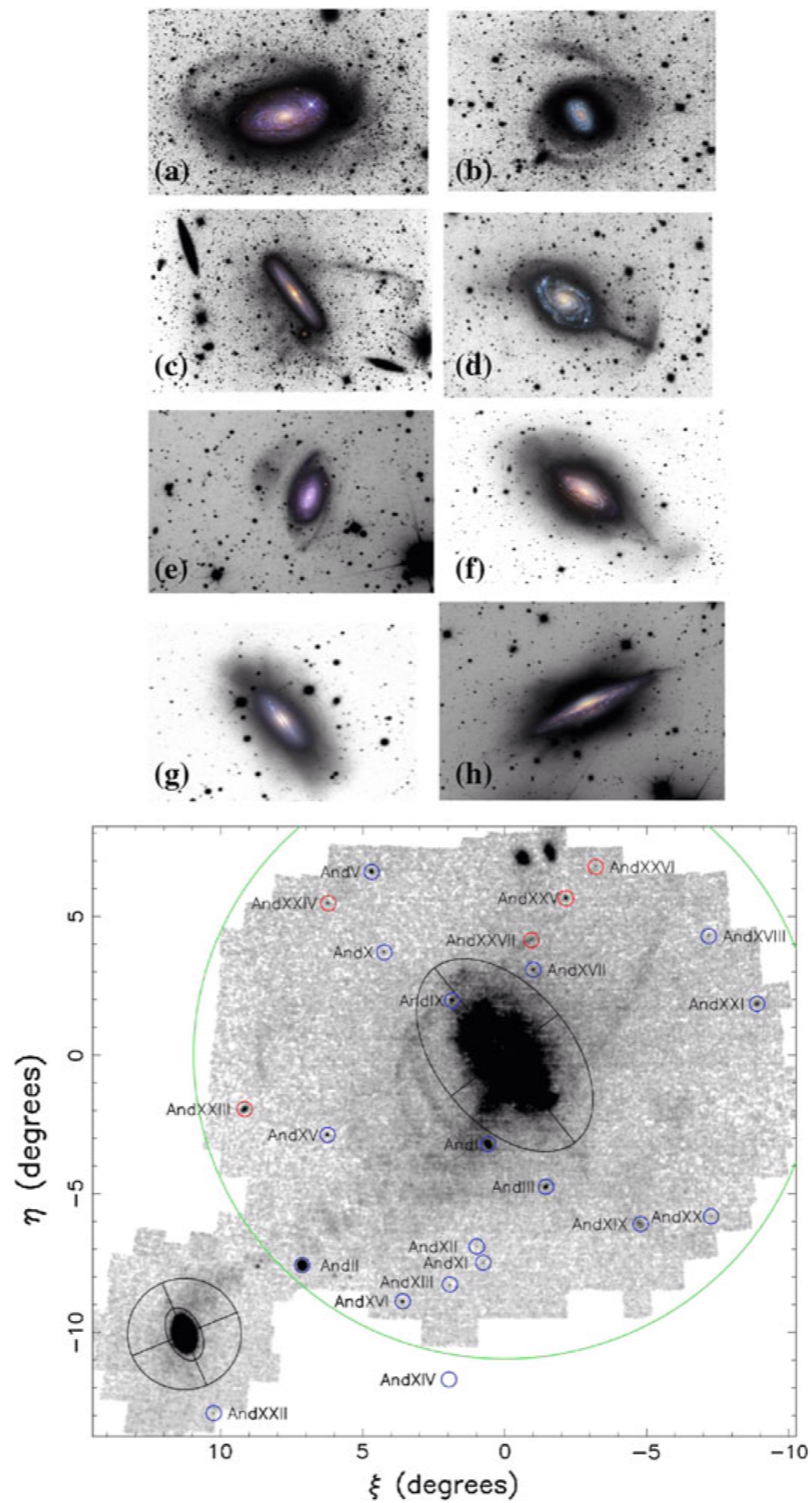


Fig. 1.20 *Upper* Examples of normal spirals with faint stellar streamers in the outer halo taken from a recent survey by Martinez-Delgado et al. [2010](#). *Lower* M31 and M33 system (PANDAs survey; Richardson et al. [2011](#)); many associated dwarfs are also shown

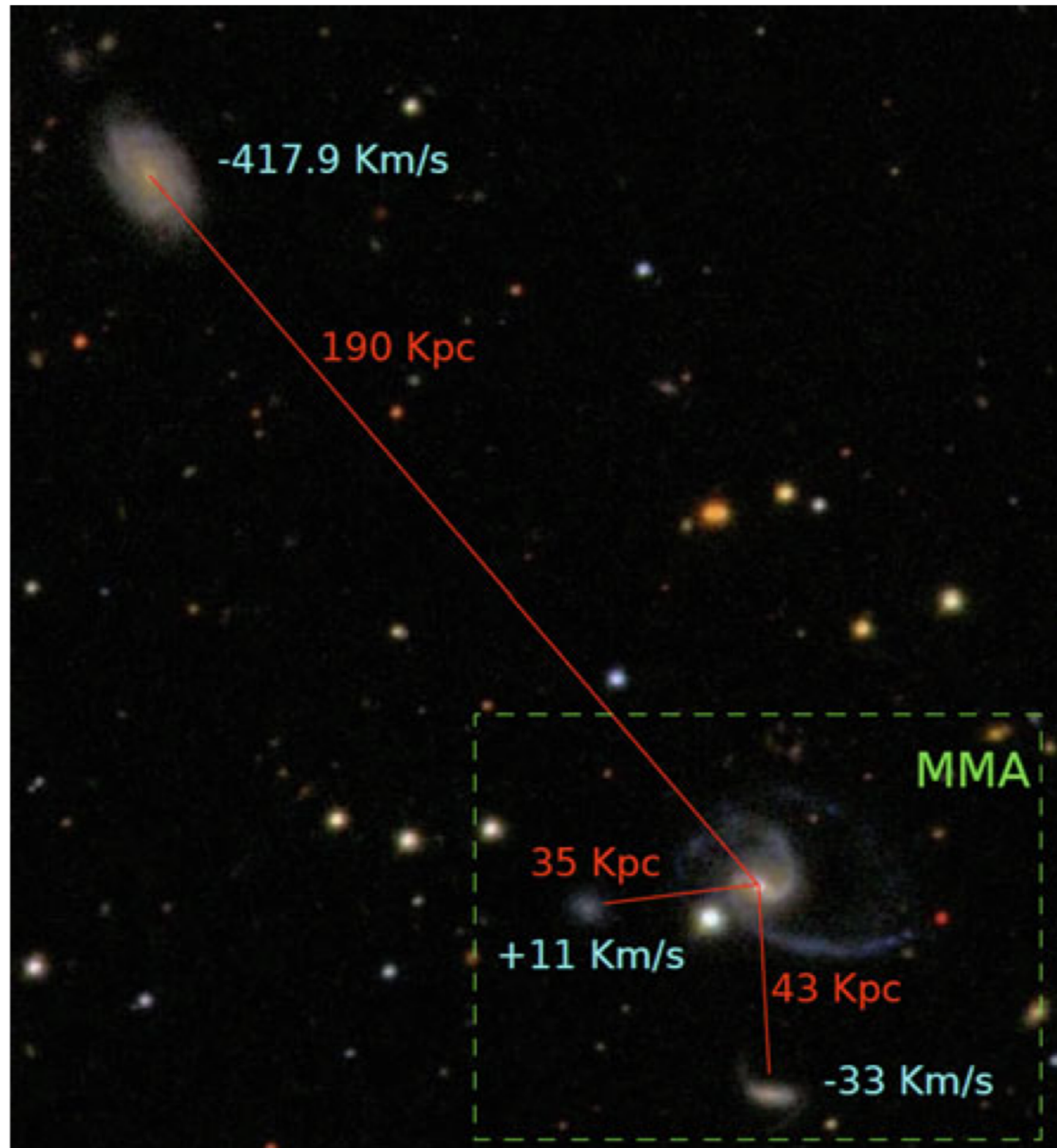
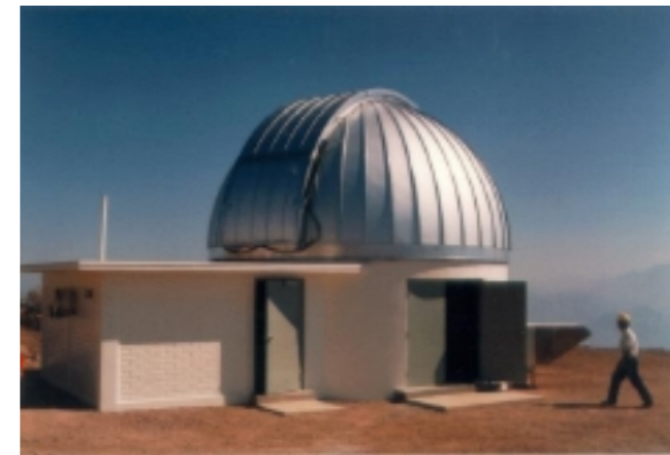


Fig. 1.9 An SDSS image of the best analogue of the Local Group to emerge from the GAMA galaxy survey (Robotham et al. [2012](#)). The group marked MMA is remarkably similar to the Milky Way—Magellanic System where the three main galaxies are all forming stars at the present time

The two 2MASS Cassegrain-focus equatorial-mount reflector telescopes are identical in construction, and each has a primary mirror diameter of 1.3 meters. One telescope is located on Mt. Hopkins in Arizona (*left*), and the other on Cerro Tololo, along the Andes mountains in Chile (facility seen at *right*). Each telescope was equipped with a three-channel camera, each channel consisting of a 256-pixel \times 256-pixel detector array, capable of observing the sky simultaneously at wavelength bands centered at wavelengths 1.25 micrometers, 1.65 micrometers, and 2.17 micrometers. (1 micrometer, abbreviated 1 μ m, is one-millionth of a meter in length.) These bands are colloquially known by astronomers as "*J*", "*H*", and "*K-short*" (or "*K_s*"). The refrigerated dewar containing the camera is the brass canister hanging below the telescope. Computers operated each telescope's motion with respect to the sky; the motion of the much-smaller secondary mirror (seen near the top of the telescope); and the dark shutters of the three channels and digital "readout" of the three detector arrays.



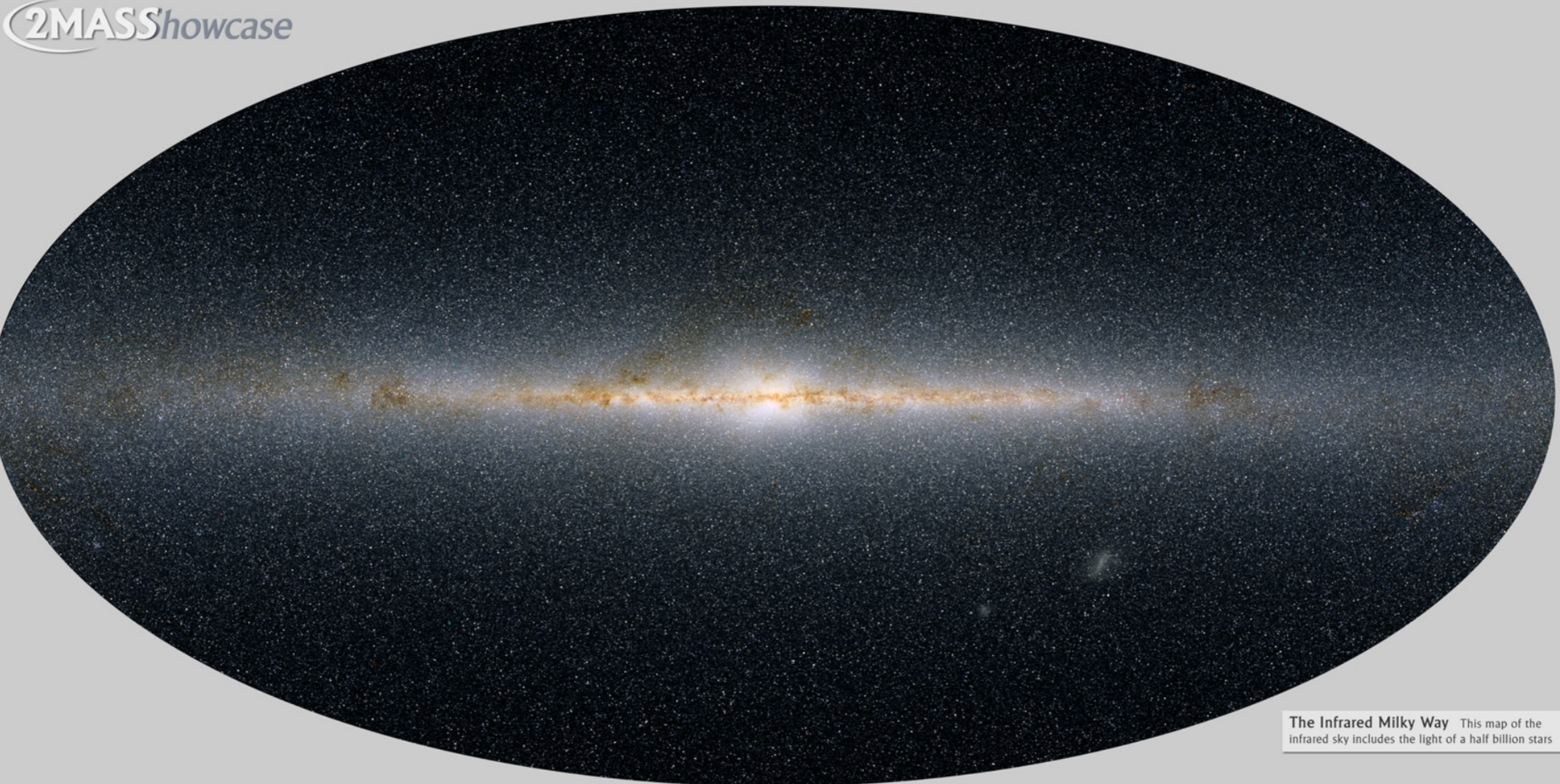
Transfer of Data from UMass to IPAC



An observing "schedule file" was sent down from UMass to the telescope operator at each of the two facilities for each night. Computers used these files to automatically control the telescopes throughout the night. The operator at each facility monitored the telescope operations and the acquiring of data. Each morning the digital data were written to magnetic tape storage, and the tapes were sent to IPAC. Each night's data were put through an automated "*pipeline*" of computer programs, which convert the raw images made by the telescopes into final *processed* images and catalogs containing star and galaxy brightnesses

and positions. These data were assessed for quality, through some human intervention. If these data passed muster, they were included as part of the enormous 2MASS *database*, from which a *digital image atlas of the sky* and *catalogs* of point sources and extended sources, freely available to astronomers and the public at large, were assembled and distributed.

2MASS Showcase



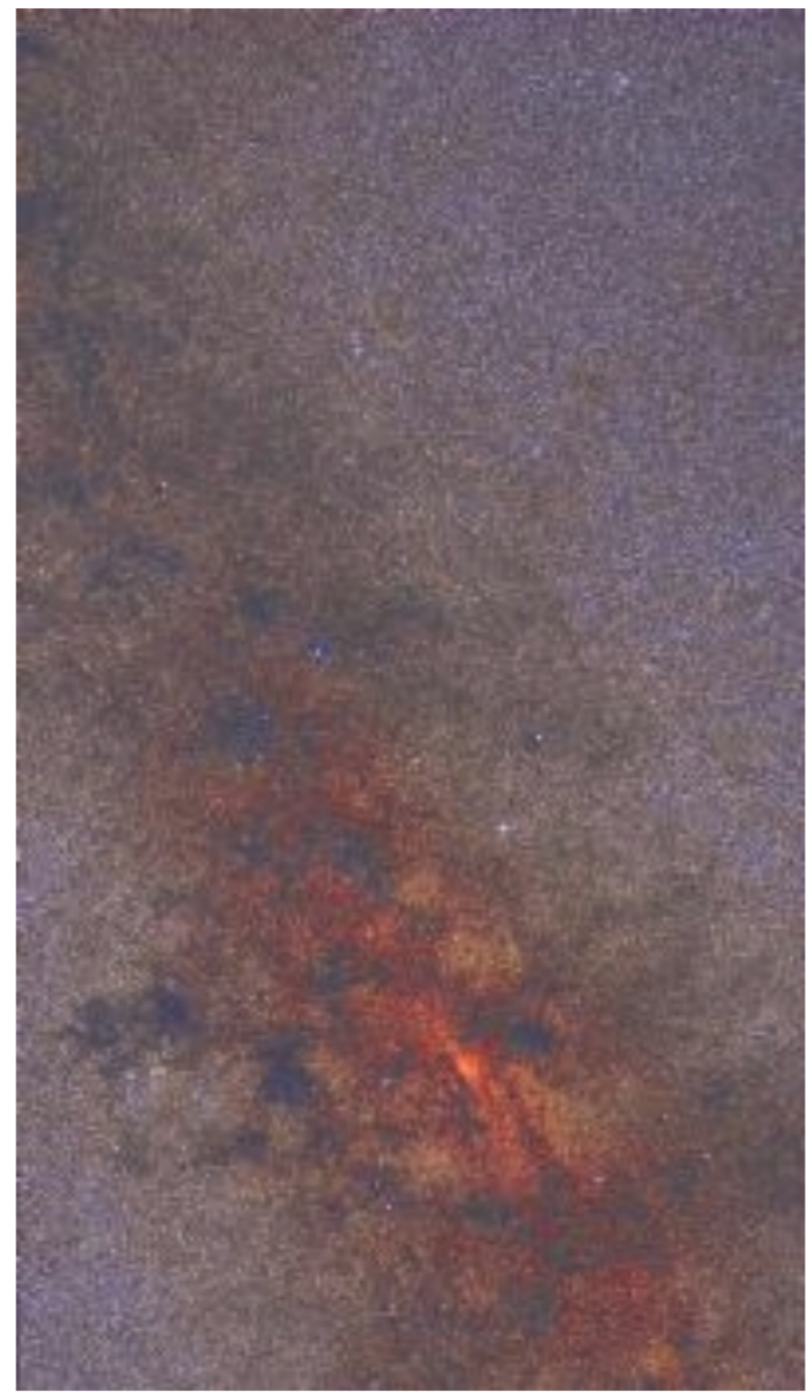
The Infrared Milky Way This map of the infrared sky includes the light of a half billion stars

POSS



Optical

2MASS

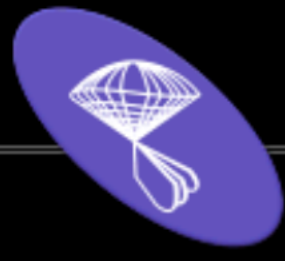


Near-Infrared

IRAS



Far-Infrared



Sloan Digital Sky Survey

Mapping the Universe

- Home
- SDSS-III
- SDSS Data DR10
- SDSS Data DR9
- SDSS Data DR8
- SDSS Data DR7
- Science
- Press Releases
- Education
- Image Gallery
- Legacy Survey
- SEGUE
- Supernova Survey
- Collaboration
- Publications
- Contact Us
- Search

The Sloan Digital Sky Survey

The Sloan Digital Sky Survey (SDSS) is one of the most ambitious and influential surveys in the history of astronomy. Over eight years of operations (SDSS-I, 2000-2005; SDSS-II, 2005-2008), it obtained deep, multi-color images covering more than a quarter of the sky and created 3-dimensional maps containing more than 930,000 galaxies and more than 120,000 quasars.

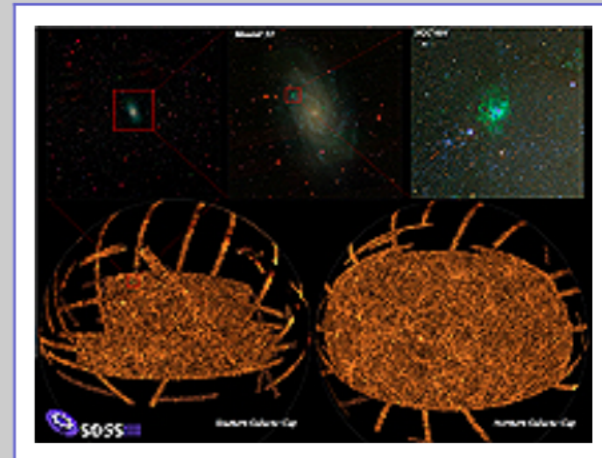
SDSS data have been released to the scientific community and the general public in annual increments, with the final public data release from SDSS-II occurring in October 2008. That release, [Data Release 7](#), is available through this website.

Meanwhile, SDSS is continuing with the [Third Sloan Digital Sky Survey \(SDSS-III\)](#), a program of four new surveys using SDSS facilities. SDSS-III began observations in July 2008 and released [Data Release 8](#) in January 2011, [Data Release 9](#) in August 2012, and [Data Release 10](#) in July 2013. SDSS-III will continue operating and releasing data through 2014.

[Data Release 10](#) contains the first release of APOGEE infrared Galactic spectroscopy as well as cumulative updates to the BOSS optical extragalactic spectroscopy archive.

[Data Release 9](#) contains the first release of BOSS spectroscopy to the public as well as

Images of the SDSS (click for more information)



The Final Survey



The Whirlpool Galaxy (M51)

Sloan Digital Sky Survey

- Új-Mexikó, 2,5m-es teleszkóp Apache Pointban
- Öt színben képalkotás több mint 100 millió égitestről
- Kb. 700 ezer spektrum galaxisokról, kvazárokról és csillagokról
- Fontos magyar résztvevők (Szalay Sándor, Csabai István és tanítványaik)



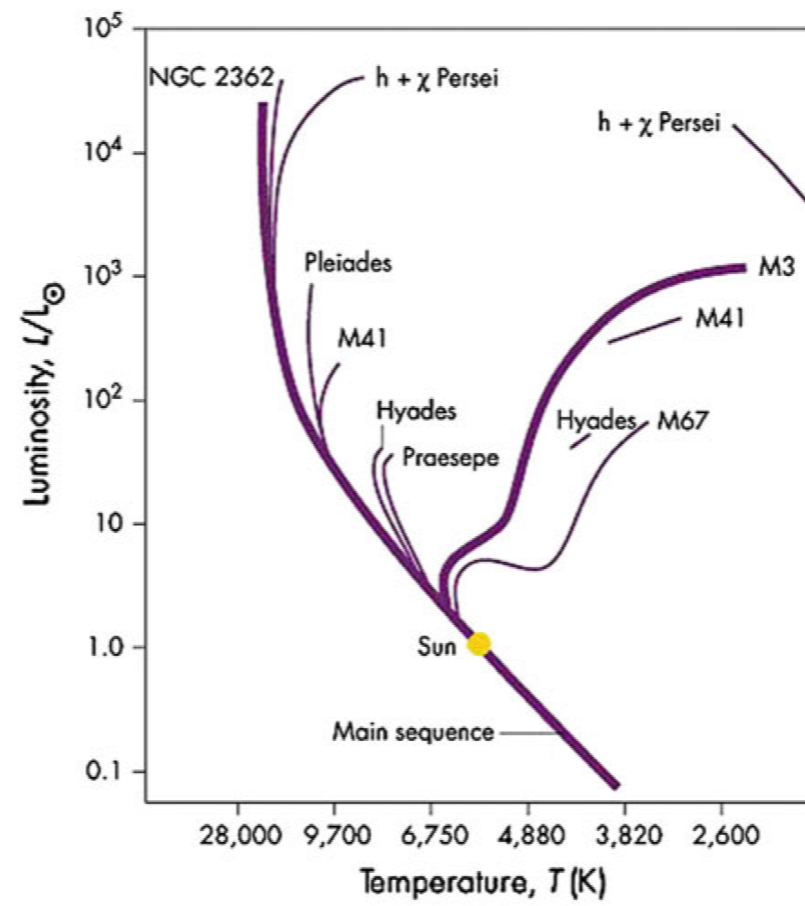


Fig. 1.21 *Upper* Hertzsprung-Russell diagram for stellar clusters over a wide range in age. *Lower* CFHT imaging of two open clusters M35 (NE) and NGC 2158 (SW) in Gemini. The young cluster M35 (NGC 2168) has a mass of roughly $2500 M_{\odot}$ and is 850 pc from the Sun. The massive cluster NGC 2158 is four times further away and about 1 Gyr old

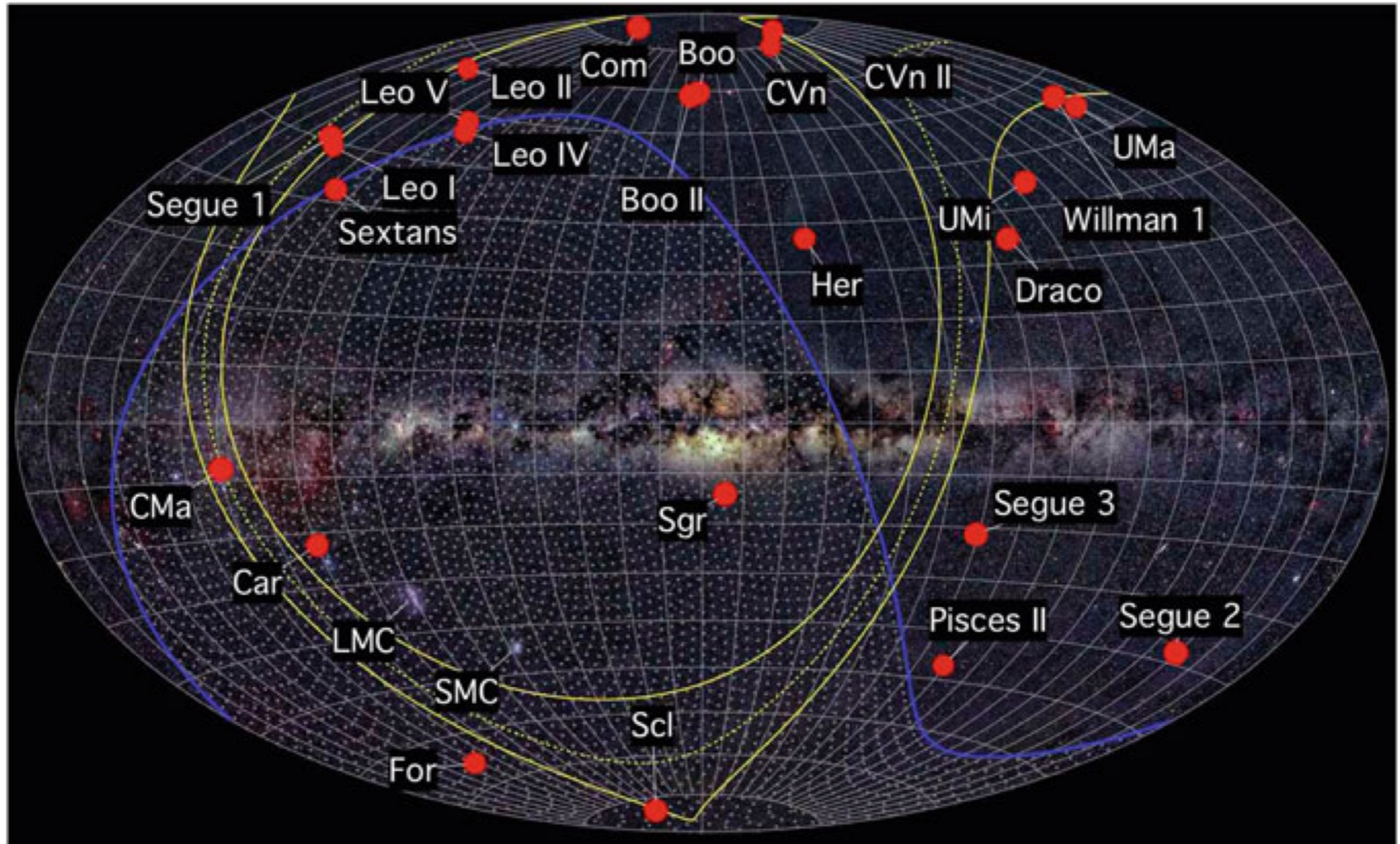


Fig. 1.22 *Upper Aitoff projection of a satellite in orbit about the Milky Way as it would appear after 8 Gyr. While stars from the disrupted satellite appear to be dispersed over a very wide region of sky, it will be possible to deduce the parameters of the original event using special techniques (see text) (we acknowledge A. Helmi and S. White for this image). Lower Aitoff projection of most of the known dwarfs in orbit about the Galaxy. For decades, astronomers have argued that these are broadly confined to a plane rather than spherically distributed, an effect that is also seen in the PANDAs survey for the dwarfs in M31 (we acknowledge A. Frebel for this image)*

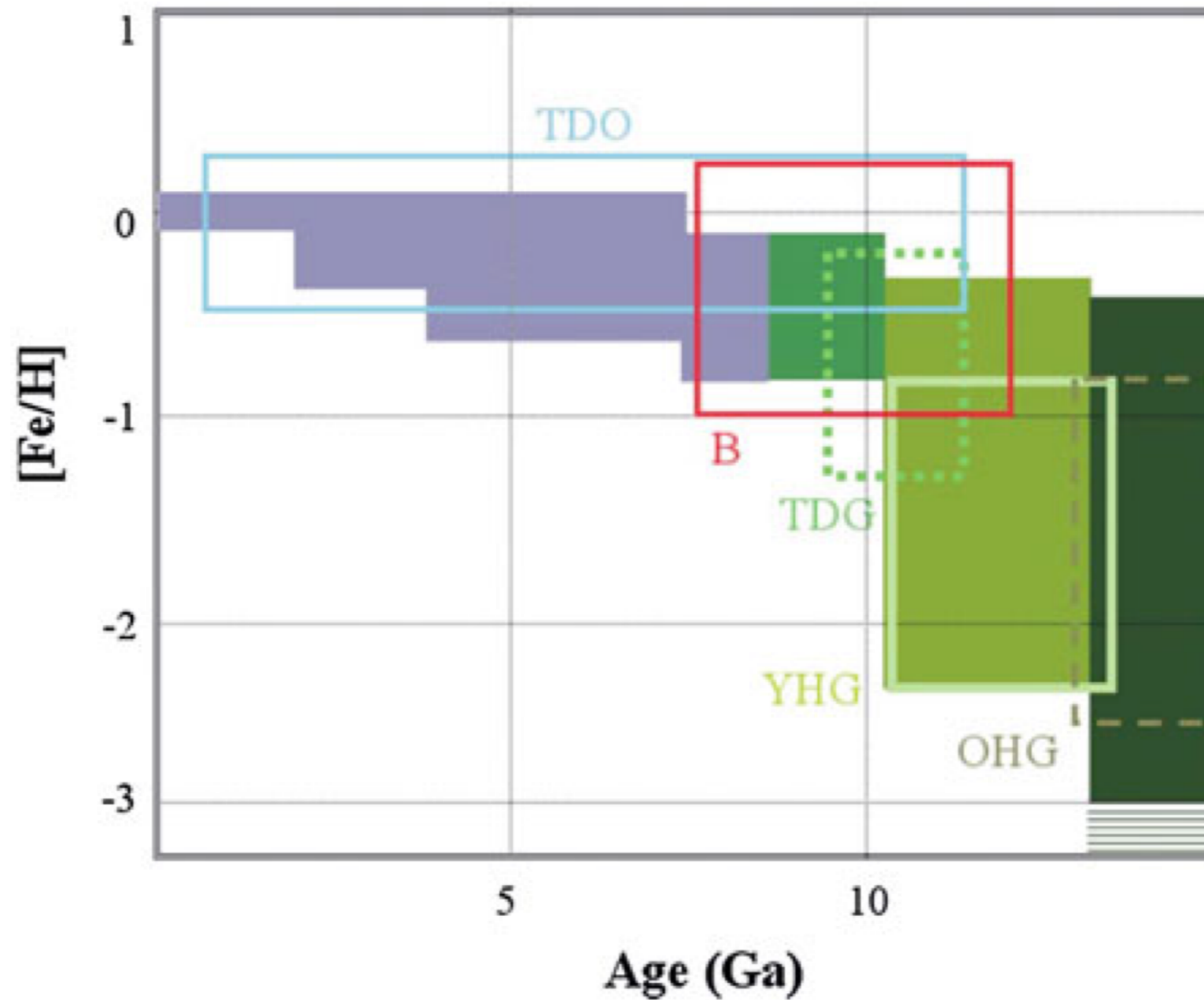


Fig. 1.16 The age-metallicity relation of the Galaxy for the different components (see text): *TDS* thin disk stars; *TDO* thin disk open clusters; *ThDS* thick disk stars; *ThDG* thick disk globulars; *B* bulge; *YHG* young halo globulars; *OHG* old halo globulars

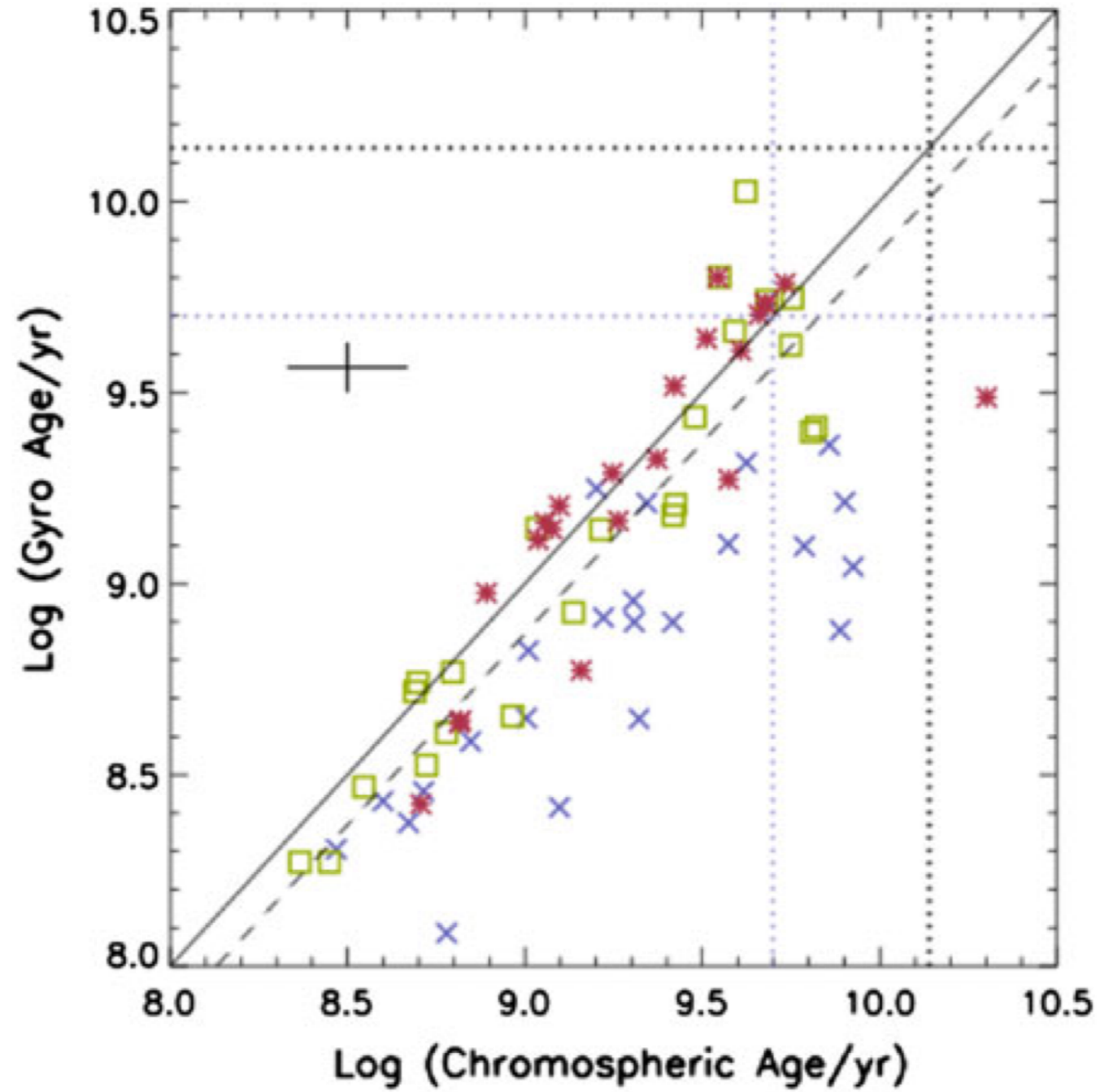


Fig. 1.17 Gyro ages versus chromospheric ages for a sample of well-studied stars (Barnes [2007](#)). The *blue crosses* are for stars bluer than $B - V = 0.6$ and should be disregarded

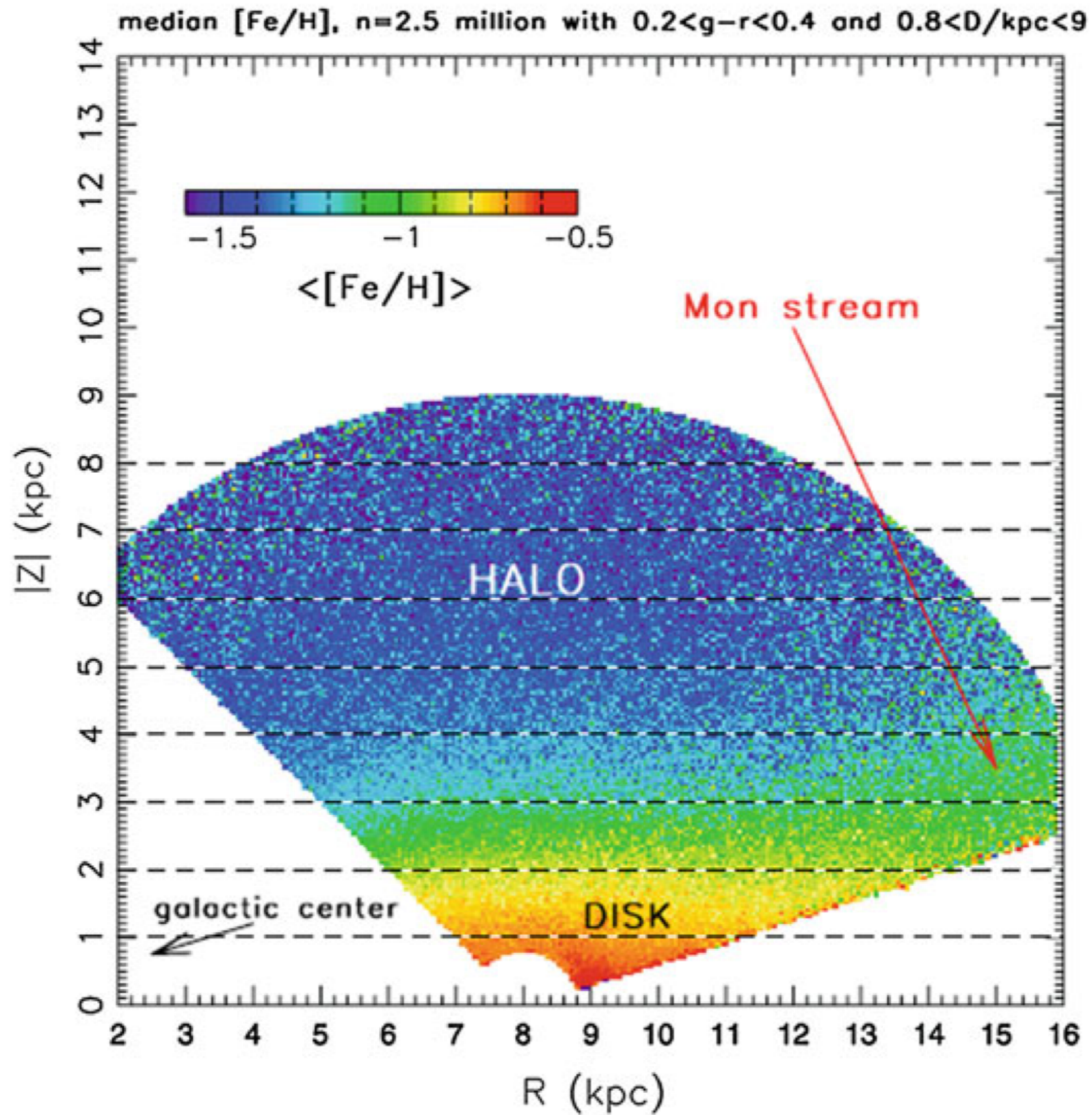
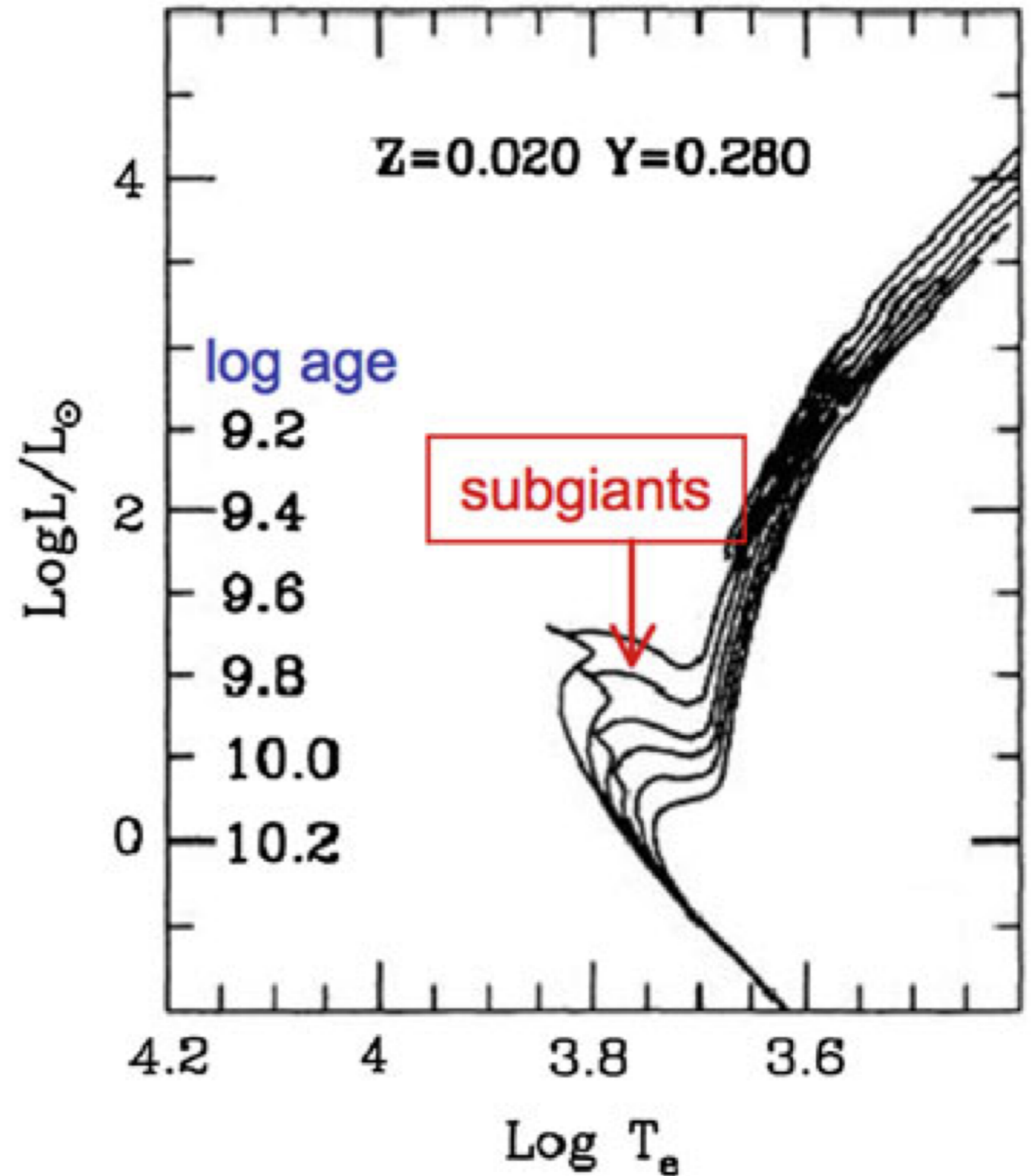


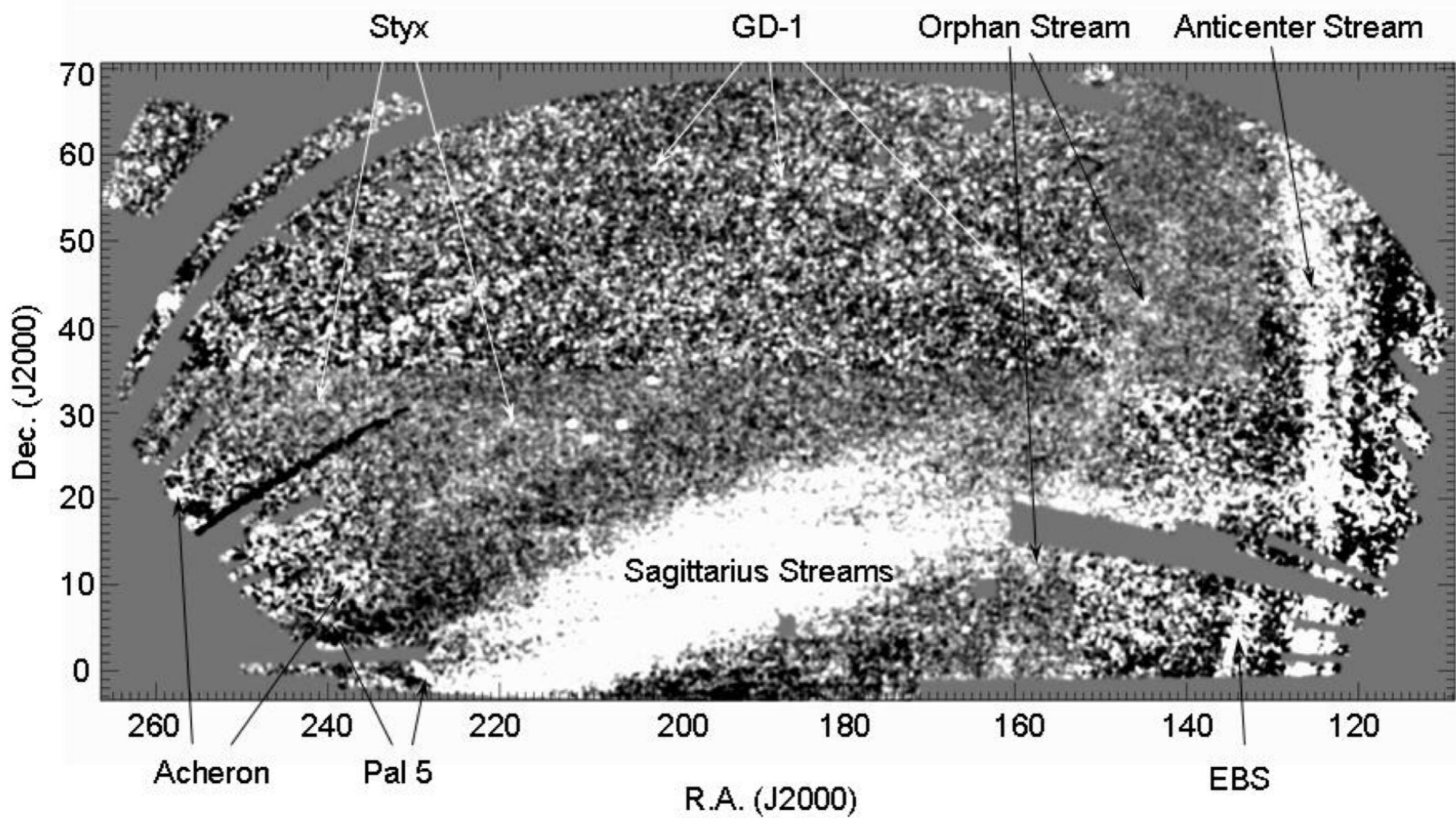
Fig. 1.32 Distribution of metallicity in the Galaxy from SDSS photometry (from Ivezić et al. [2008](#))

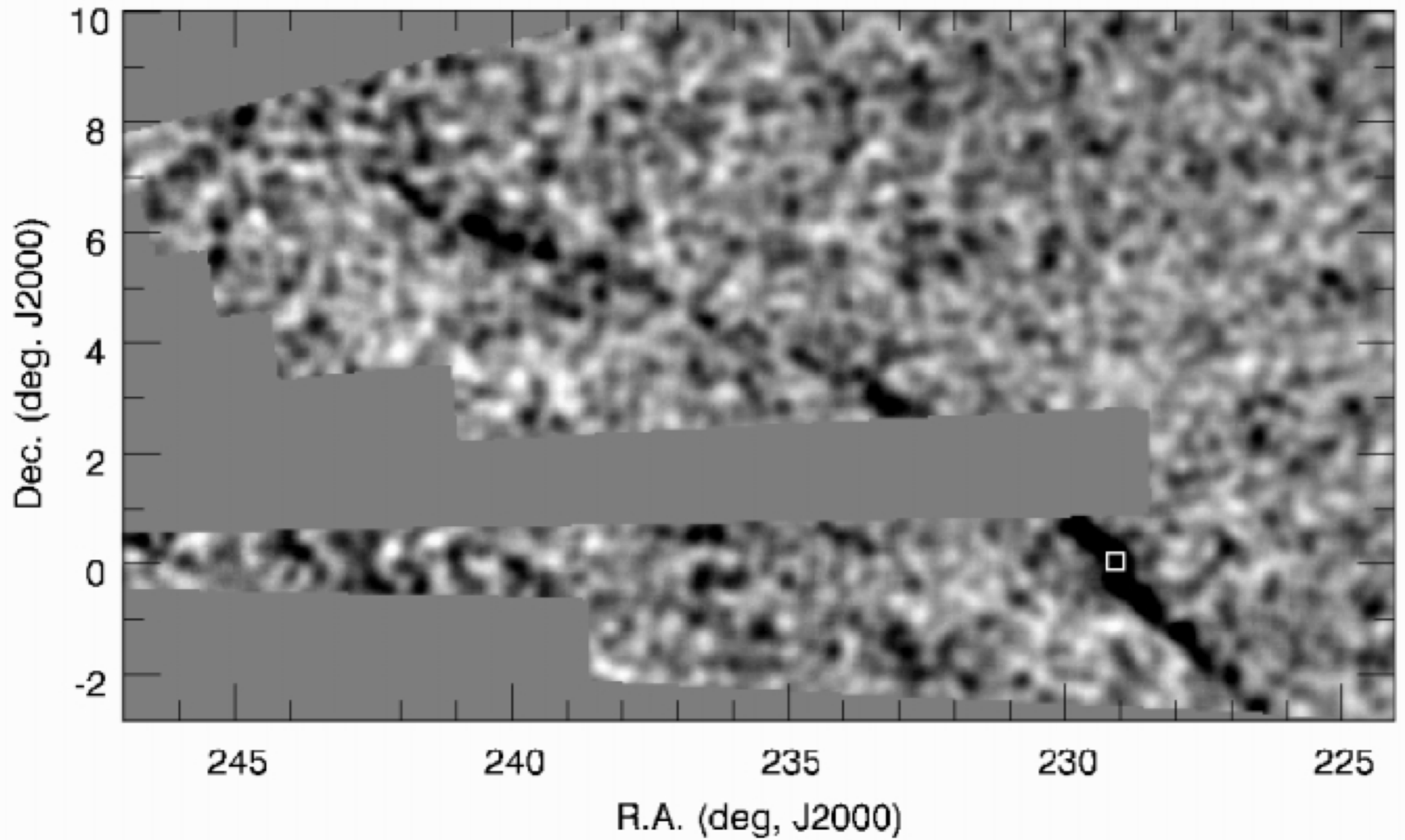
Fig. 1.39 Isochrones from Bertelli et al. (1994) for stars of near-solar abundance and a range of ages from 1.6 to 16 Gyr. The isochrones can overlap near the turnoff but are well separated in the subgiant region



**Table 1** Known Distant Galactic Streams

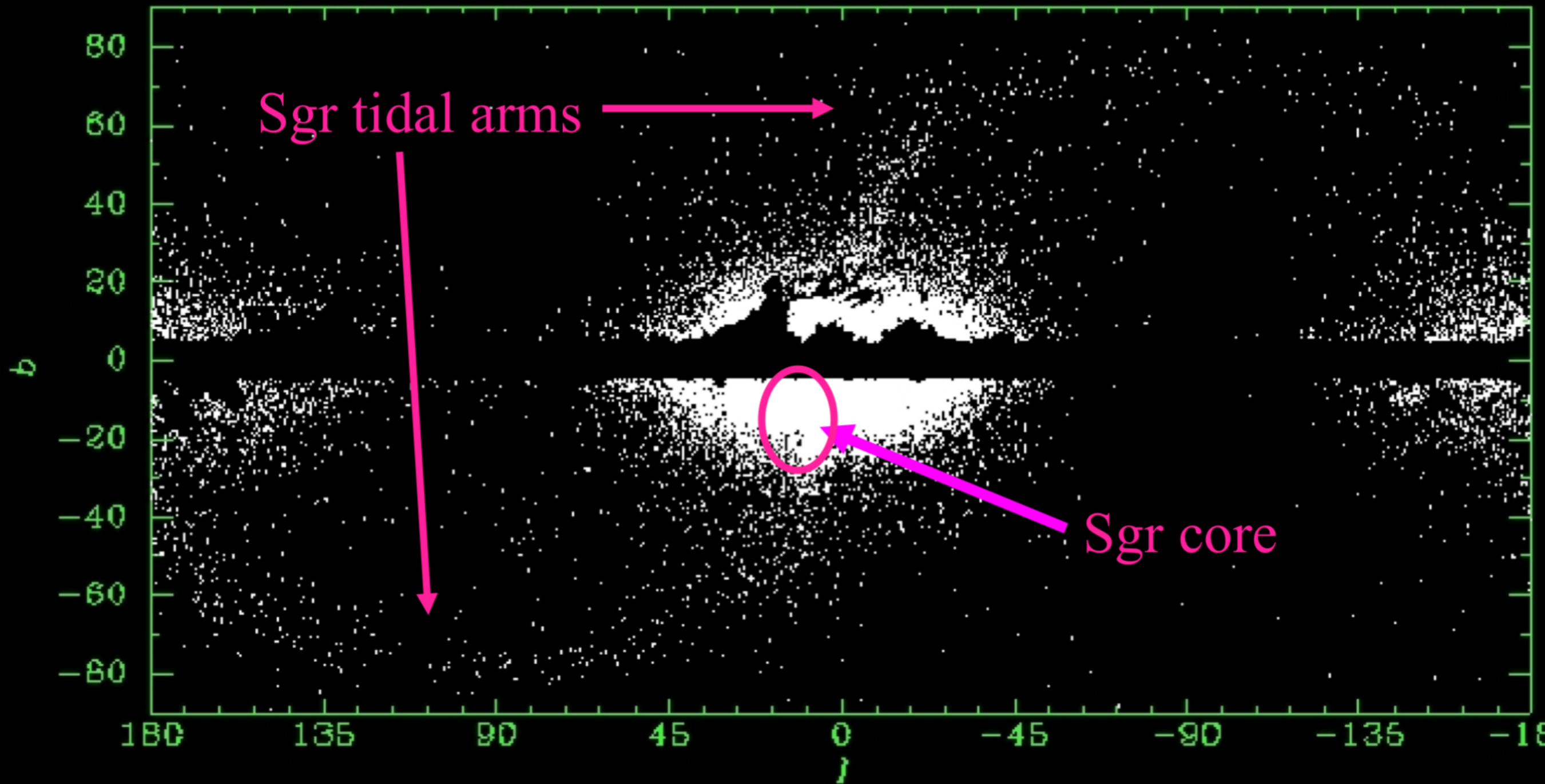
Designation	Progenitor	Selected References
Sagittarius	Sagittarius Dwarf Galaxy	Ibata et al. 1994, Mateo et al. 1996, Alard 1996, Toten & Irwin, 1998, Ibata et al. 2001, Martinez-Delgado et al. 2004, Majewski et al. 2004, Vivas et al. 2005, Belokurov et al. 2006b, Fellhauer et al. 2006, Bellazzini et al. 2006, Chou, M-Y et al. 2007, Law et al. 2009
Virgo Stellar Stream	NGC 2419?	Vivas et al. 2001, Duffau et al, 2006, Newberg et al. 2007
Palomar 5	Palomar 5	Odenkirchen et al. 2001, 2003, 2009, Rockosi et al. 2002, Grillmair & Dionatos 2006b
Monoceros Ring	Unknown (dwarf galaxy?)	Newberg et al. 2002, Yanny et al. 2003, Ibata et al. 2003, Rocha-Pinto et al. 2003, Penarrubia et al. 2005
NGC 5466	NGC 5466	Belokurov et al. 2006a, Grillmair & Johnson 2006, Fellhauer 2007
Orphan Stream	Unknown (dwarf galaxy?)	Grillmair 2006a, Belokurov 2007, Fellhauer et al. 2007, Sales et al. 2008, Newberg et al. 2010
GD-1	Unknown (globular cluster?)	Grillmair & Dionatos 2006b, Willet et al. 2009, Koposov, Rix, & Hogg 2009
AntiCenter Stream	Unknown (dwarf galaxy?)	Grillmair 2006b, Grillmair, Carlin, & Majewski 2008
EBS	Unknown (dwarf galaxy?)	Grillmair 2006, Grillmair, Carlin, & Majewski 2008
Acheron	Unknown (globular cluster?)	Grillmair 2009
Cocytos	Unknown (globular cluster?)	Grillmair 2009
Lethe	Unknown (globular cluster?)	Grillmair 2009
Styx	Bootes III dwarf?	Grillmair 2009
Cetus Polar Stream	NGC 5824?	Newberg, Yanny, & Willett 2009

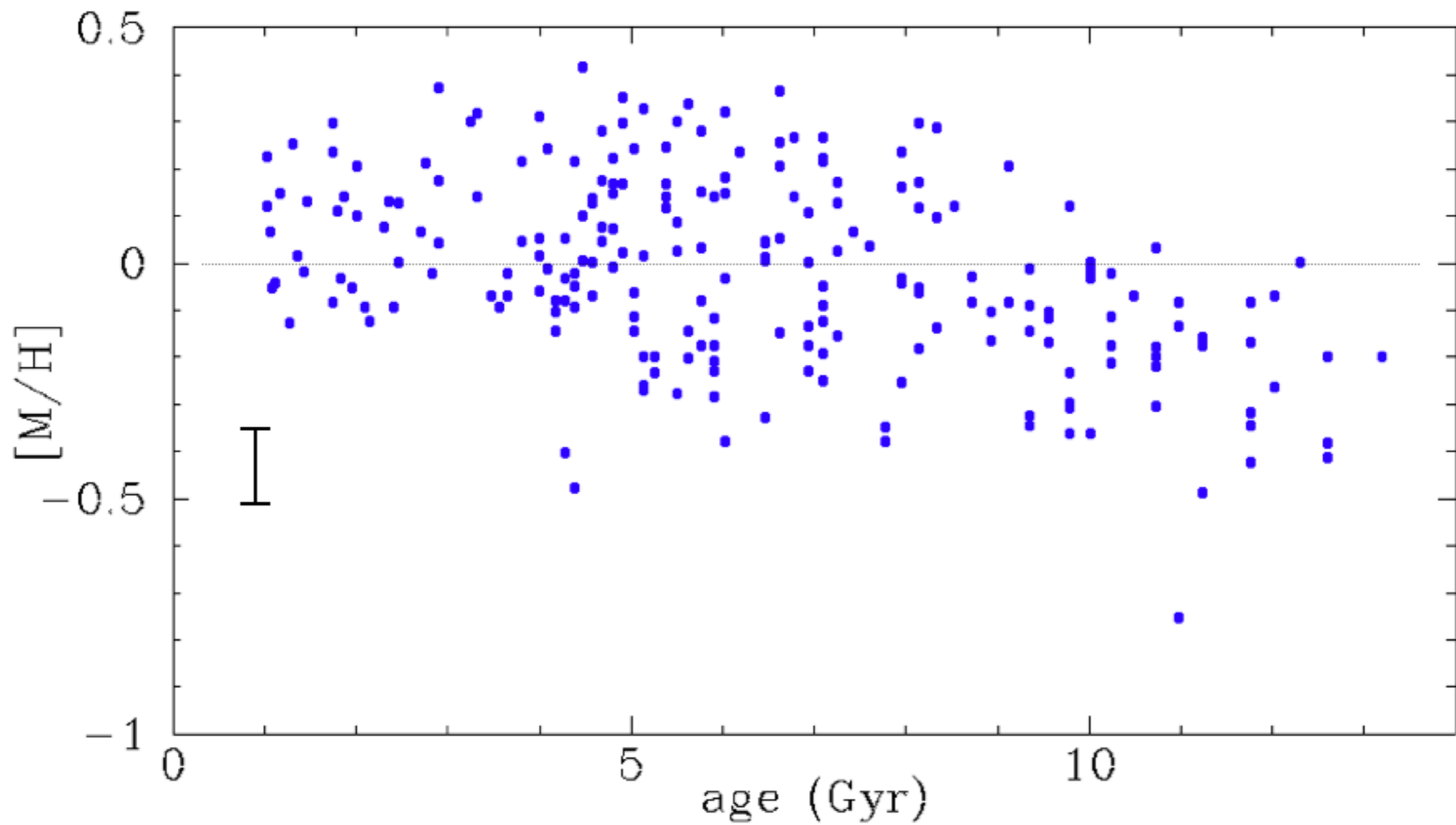




Grillmair & Dionatos 2006

All-sky view of 2MASS M giant star distribution





1: The age-metallicity relation for subgiants near the sun (Wylie de Boer & Freeman 1999, unpublished). The estimated random errors in $[M/H]$ are shown by the error bar. The random errors in age are believed to be about 30%.

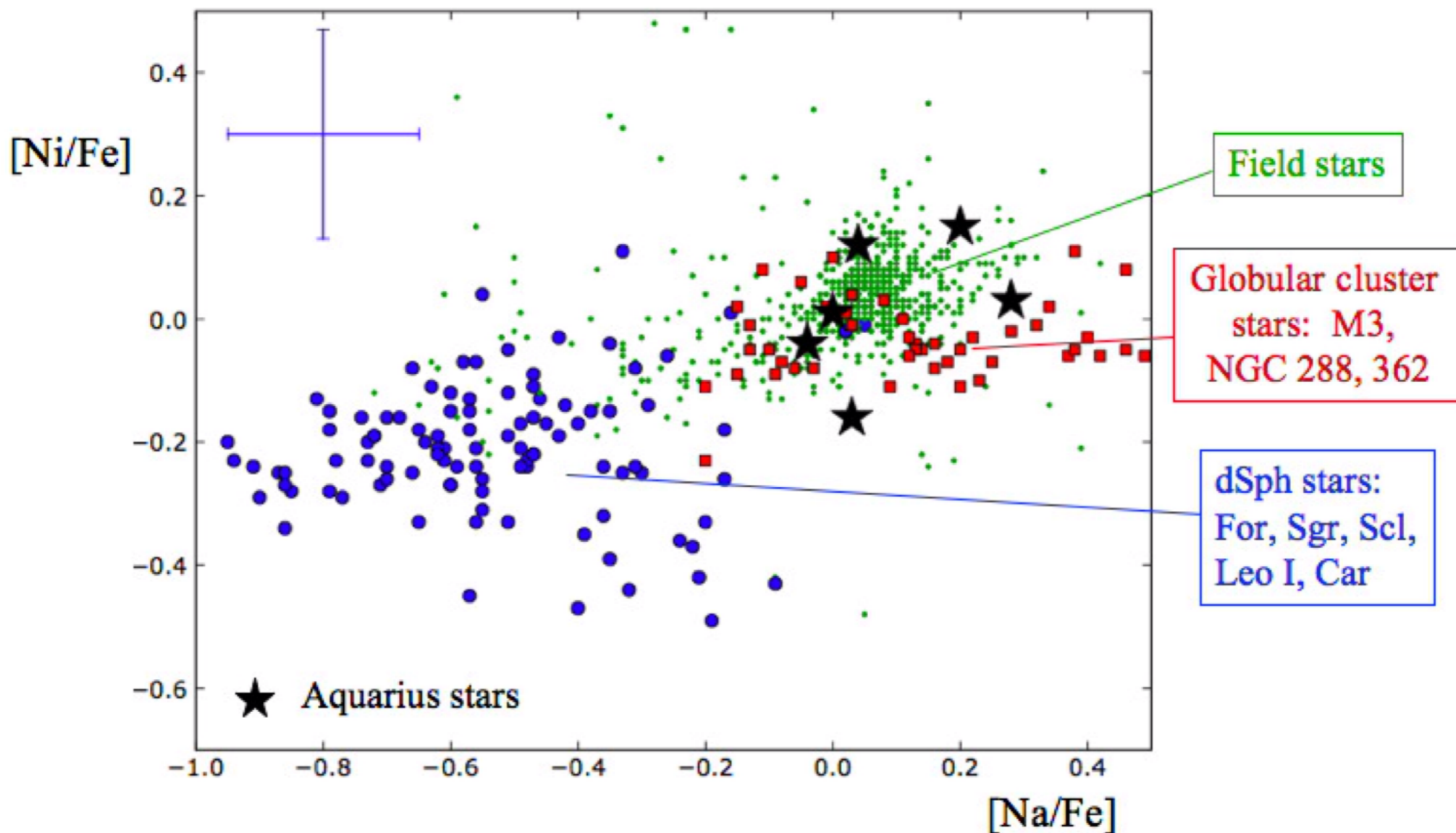
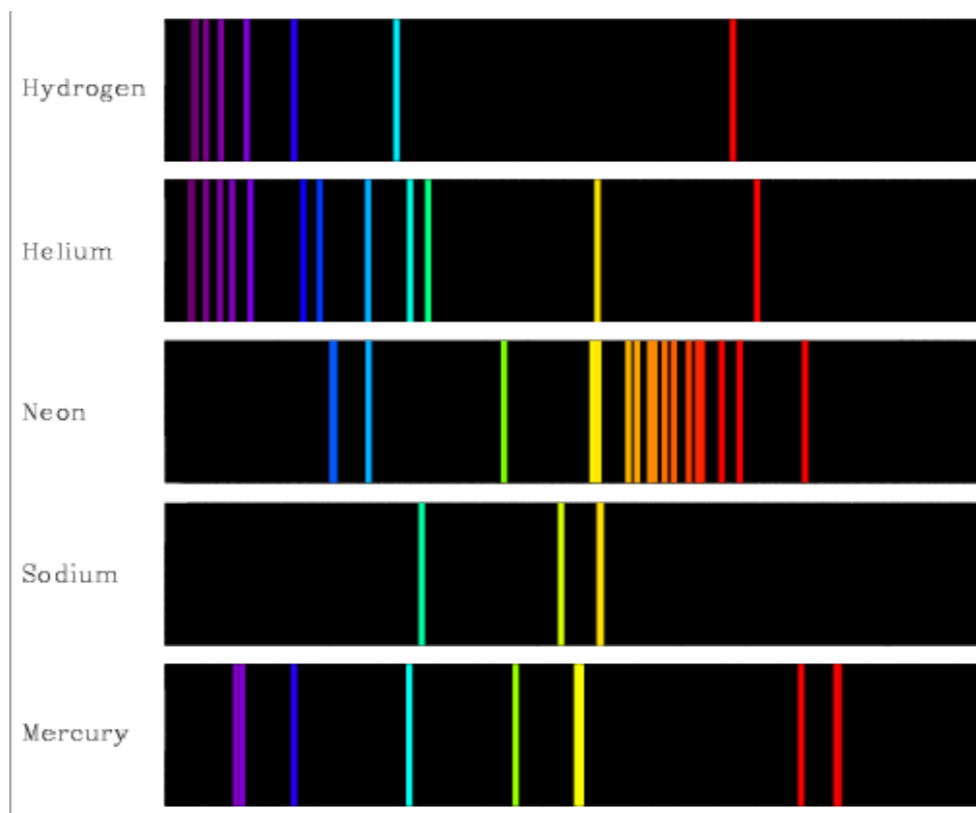
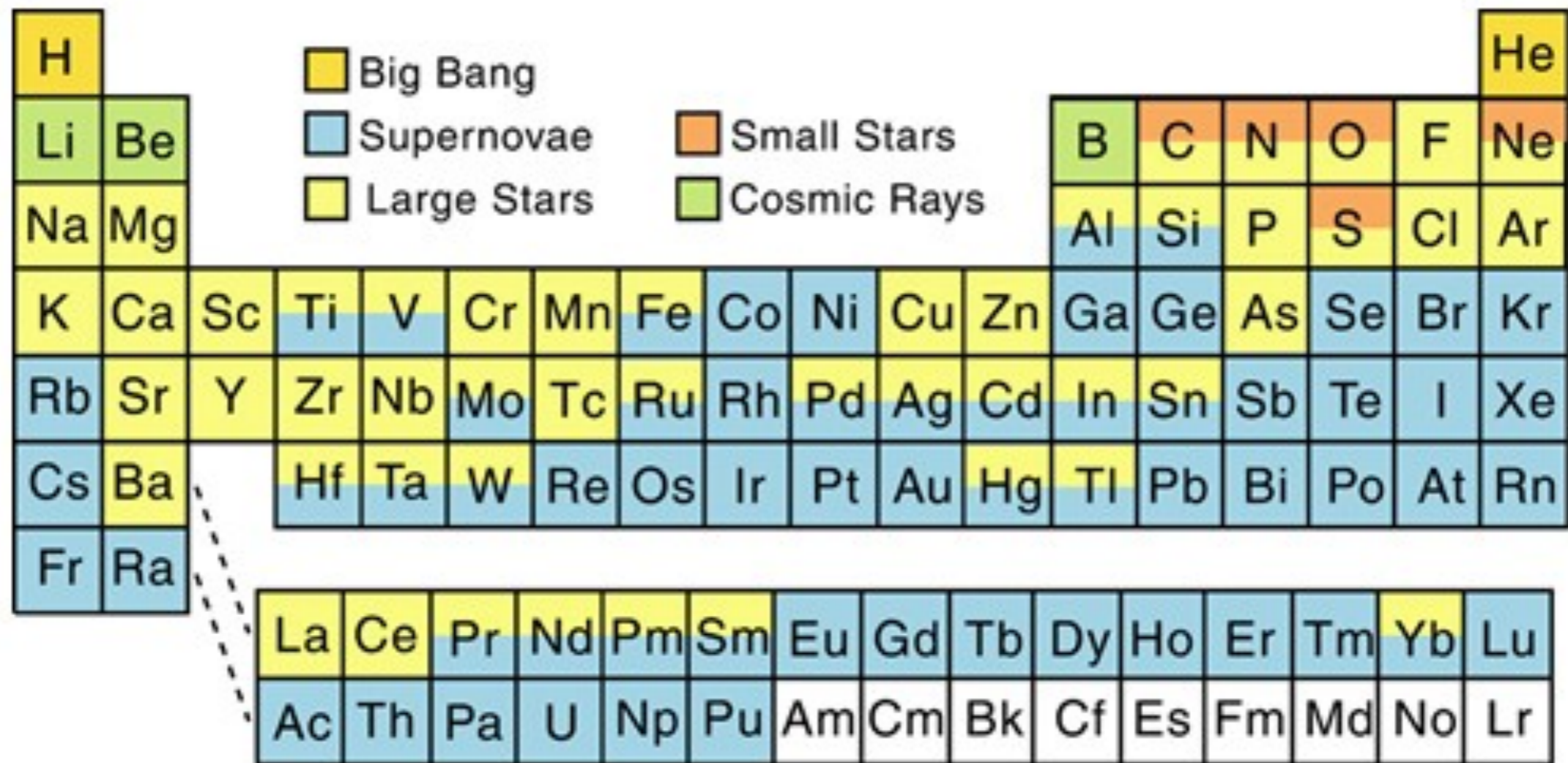


Figure 4: The Na-Ni distribution for globular cluster stars, dwarf spheroidal galaxy stars, field halo stars and stars of the Aquarius stream (black star symbols) (Wylie de Boer et al. 2012). The stars of the Aquarius stream are in the same part of the distribution as the globular cluster stars.

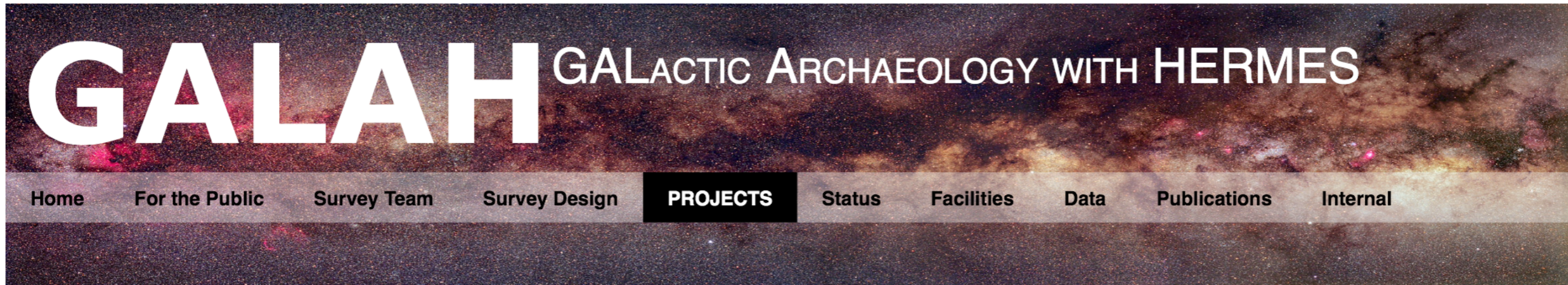
galaxies. The distribution of their stars in the $[X/Fe]$ - $[Fe/H]$ plane is well defined for an individual galaxy but differs in structure from galaxy to galaxy depending on their star formation history





MOS with multiplex > 300

Project	Hemisphere	Tel. diam. (m)	FOV (sq deg)	Fibres / slits	Spectroscopic resolution	First light
AAT / AAOmega	S	3.9	3.14	392 fibres	1300 - 8000	2006
AAT / Hermes	S	3.9	3.14	400 fibres	28000	2012
CFHT / GYES	N	3.6	0.64	500 fibres	20000	Proposed
CTIO Blanco / DESpec	S	4.0	3.8	4000 fibres	2000	2012
GTC / GO-IRS	N	10.4	0.05	1000 fibres	5000 - 20000	2013
LAMOST	N	4.0	19.63	4000 fibres	1000, 10000	2009
Mayall / BigBOSS	N	3.8	7.07	5000 fibres	3000 - 4000	2016
MMT / HECTOSPEC	N	6.5	0.79	300 fibres	1000	2003
NTT or VISTA / 4MOST	S	4	7.1	3000 fibres	3000 - 5000	2017 - 2018
SDSS-III / BOSS	N	2.5	7.07	1000 fibres	1600 - 2700	2009
Subaru / PFS	N	8.2	1.78	2400 fibres	2000 - 5000	-
VLT / MOONS	S	8.2	0.14	500 fibres	3000 - 20000	2017
WHT / WEAVE	N	4.2	3.14	1000 fibres	5000, 20000	2016



Scientific Goals

- Changes with Time
- Accretion History
- Dynamics
- Nucleosynthetic Processes

Pilot Studies

Collaborative Work

- APOGEE
- CoRoT
- Gaia
- Gaia-ESO
- Kepler
- RAVE
- SkyMapper

With GALAH, we will chemically tag stars into coeval groups, identifying individual members of star clusters which have long since dispersed. Using the stellar relics of ancient star formation and accretion events, we can reconstruct the Galactic accretion history, and dynamical and chemical evolution.

The GALAH data sets will yield a comprehensive view of the formation and evolution of the Milky Way disk and address the following basic questions:

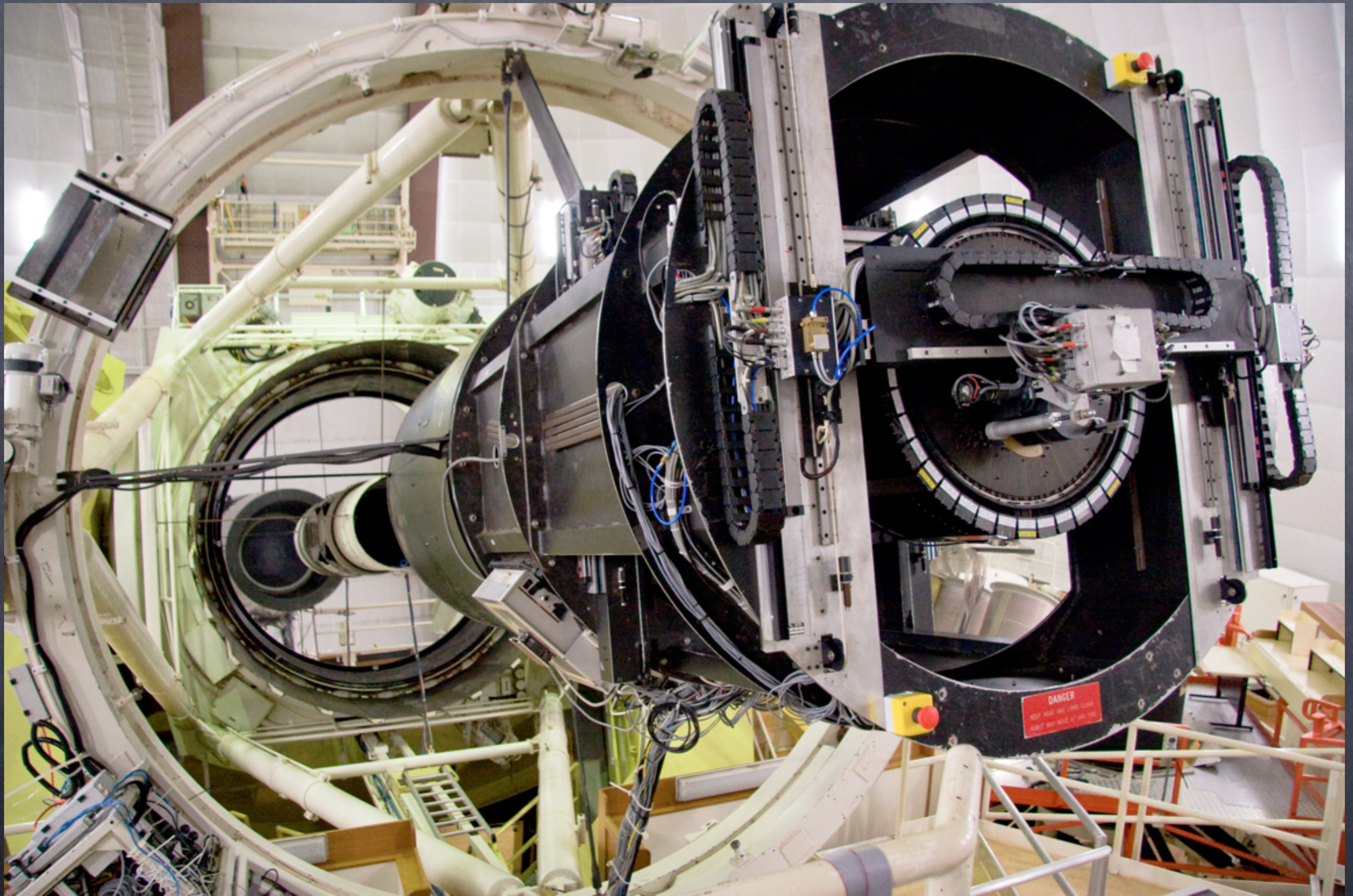
- What were the conditions of star formation during early stages of Galaxy assembly?
- When and where were the major episodes of star formation in the disk and what drove them?
- To what extent is the Galactic disk composed of stars from merger events?
- Under what conditions and in what types of systems did accreted stars form?
- How have the stars that formed *in situ* in the disk evolved dynamically since their birth?
- Where are the solar siblings that formed together with our Sun?

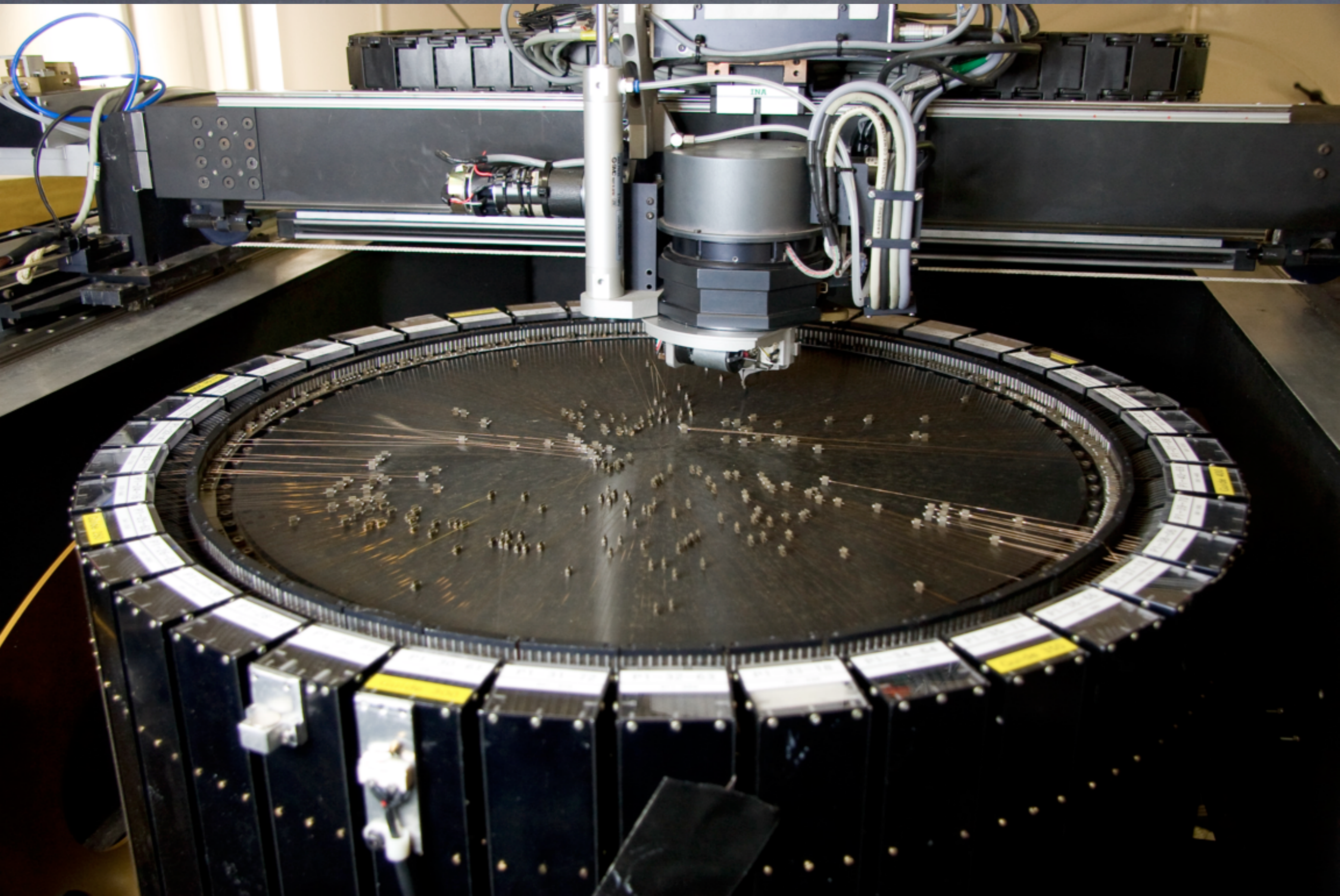
Our current priority is small scale projects that will allow us to test the HERMES instrument.

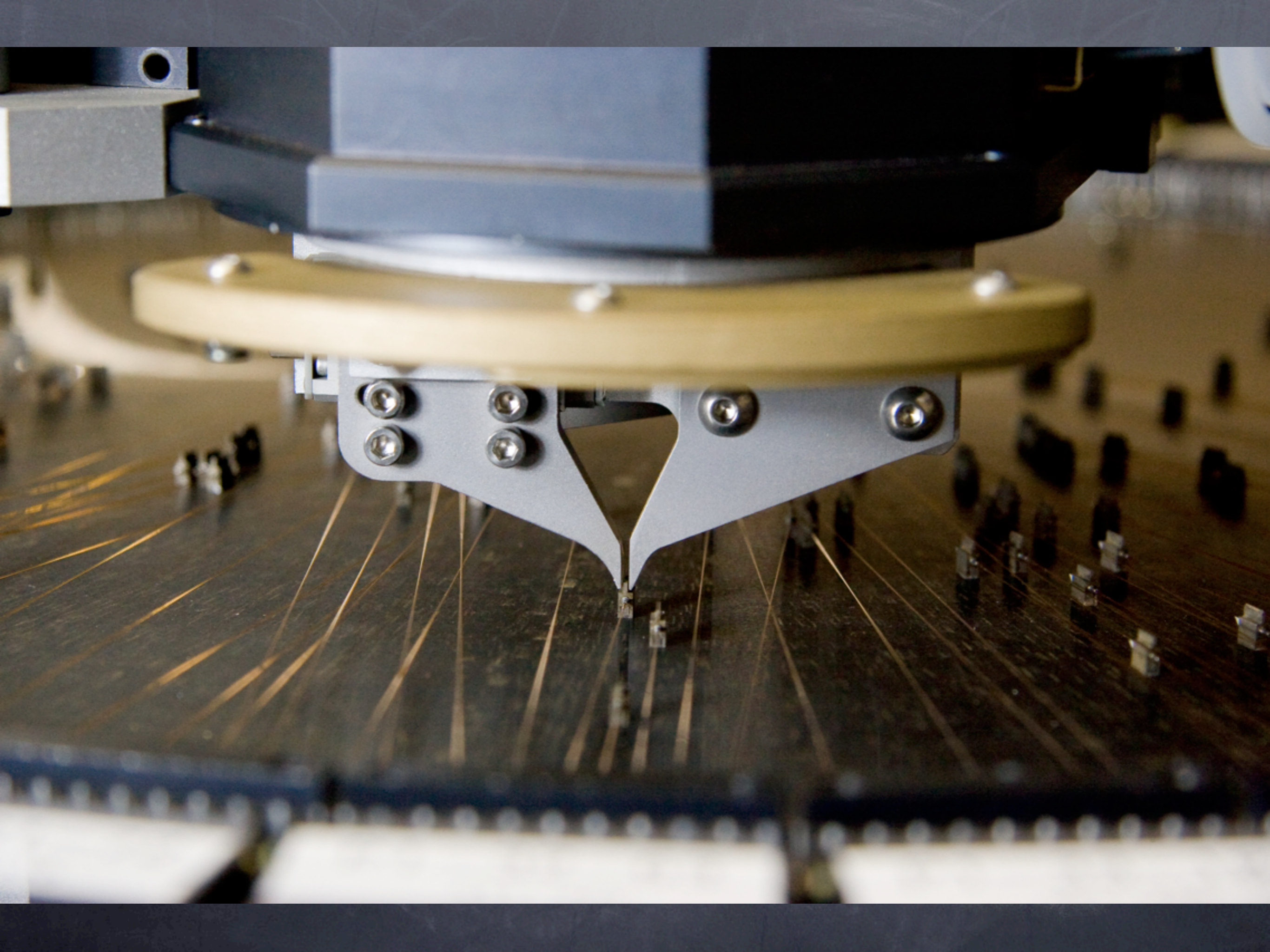
Scientific Goals

After their birth-clusters or birth-galaxies disperse, stars may change their dynamical behavior thanks to mechanisms like heating and radial migration. However, the chemical composition of these stars, which reflect the conditions of









AAOMEGA OBSERVATIONS OF 47 TUCANAE: EVIDENCE FOR A PAST MERGER?

RICHARD R. LANE¹, BRENDON J. BREWER², LÁSZLÓ L. KISS^{1,3}, GERAINT F. LEWIS¹, RODRIGO A. IBATA⁴, ARNAUD SIEBERT⁴,
TIMOTHY R. BEDDING¹, PÉTER SZÉKELY⁵, AND GYULA M. SZABÓ³

¹ Sydney Institute for Astronomy, School of Physics, A28, The University of Sydney, NSW 2006, Australia

² Department of Physics, University of California, Santa Barbara, CA 93106-9530, USA

³ Konkoly Observatory of the Hungarian Academy of Sciences, P.O. Box 67, H-1525, Budapest, Hungary

⁴ Observatoire Astronomique, Université de Strasbourg, CNRS, 67000 Strasbourg, France

⁵ Department of Experimental Physics, University of Szeged, Szeged 6720, Hungary

Received 2009 November 21; accepted 2010 February 3; published 2010 February 23

ABSTRACT

The globular cluster 47 Tucanae (47 Tuc) is well studied but it has many characteristics that are unexplained, including a significant rise in the velocity dispersion profile at large radii, indicating the exciting possibility of two distinct kinematic populations. In this Letter, we employ a Bayesian approach to the analysis of the largest available spectral data set of 47 Tuc to determine whether this apparently two-component population is real. Assuming the two models were equally likely before taking the data into account, we find that the evidence favors the two-component population model by a factor of $\sim 3 \times 10^7$. Several possible explanations for this result are explored, namely, the evaporation of low-mass stars, a hierarchical merger, extant remnants of two initially segregated populations, and multiple star formation epochs. We find the most compelling explanation for the two-component velocity distribution is that 47 Tuc formed as two separate populations arising from the same proto-cluster cloud which merged $\lesssim 7.3 \pm 1.5$ Gyr ago. This may also explain the extreme rotation, low mass-to-light ratio, and mixed stellar populations of this cluster.

Key words: globular clusters: individual (47 Tucanae)

Online-only material: color figure

1. INTRODUCTION

estimates, the membership selection process, and statistical analysis of cluster membership for all data presented in this

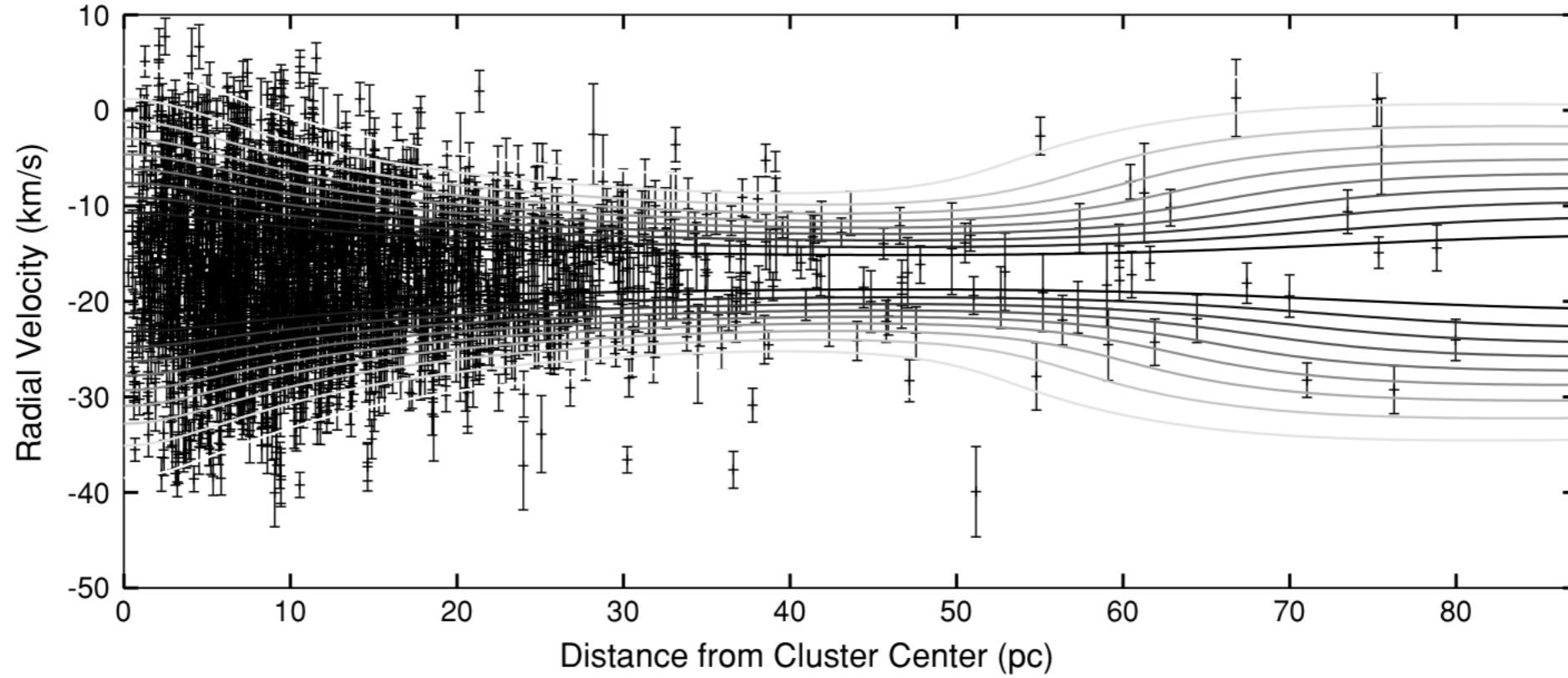


Figure 1. Radial velocities of stars in 47 Tuc together with the best-fit double Plummer model for the velocity distribution as a function of radius. The inner part of the cluster is well modeled by the dominant Plummer profile, while at larger radii, the second plummer profile dominates. The radius at which the two profiles have equal weight is 55 pc.

Table 1

Inferred Parameter Values for the Single Plummer and the Double Plummer Fits to the 47 Tuc Data

Parameter	Value
Single Plummer Profile	
μ	$-16.87 \pm 0.17 \text{ km s}^{-1}$
σ_0	$9.37 \pm 0.32 \text{ km s}^{-1}$
r_0	$9.27 \pm 0.98 \text{ pc}$
$\log(\text{evidence})$	-7759.5
Double Plummer Profile	
μ	$-16.94 \pm 0.12 \text{ km s}^{-1}$
σ_0	$9.93 \pm 0.43 \text{ km s}^{-1}$
	$[5.70, 13.51] \pm \text{ km s}^{-1}$

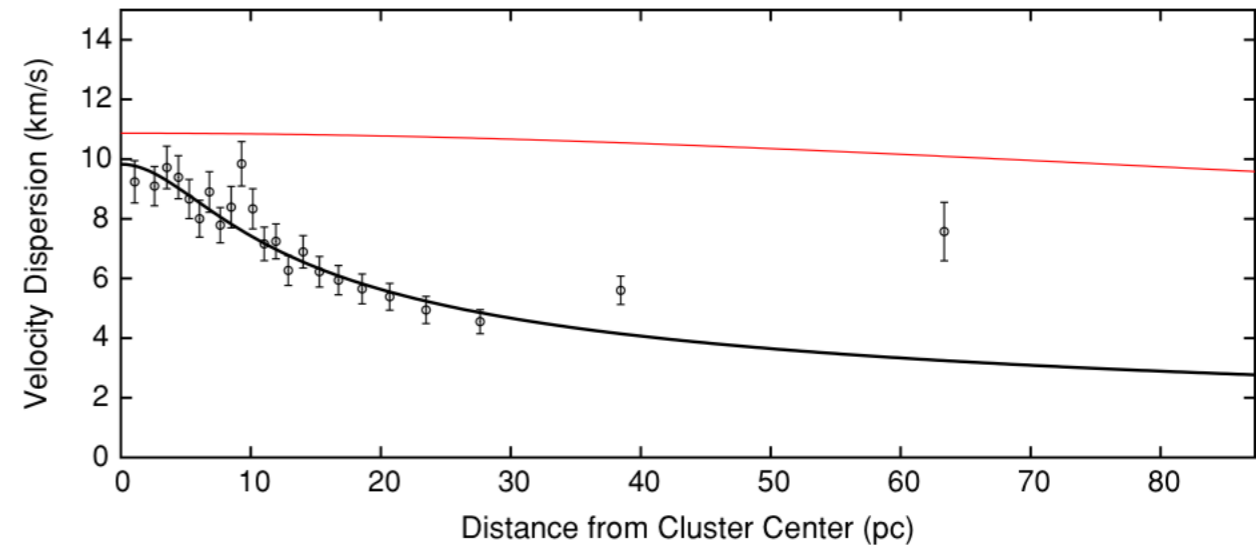


Figure 2. Binned velocity dispersion as a function of radius (from Lane et al. 2010a), with the radial velocity profiles of the two stellar populations from the best-fit double Plummer model. The Plummer profile that dominates at small radii is shown as the thick (black) curve; the thin (red) curve shows the Plummer



WEAVE

A new wide-field multi-object spectrograph for the William Herschel Telescope



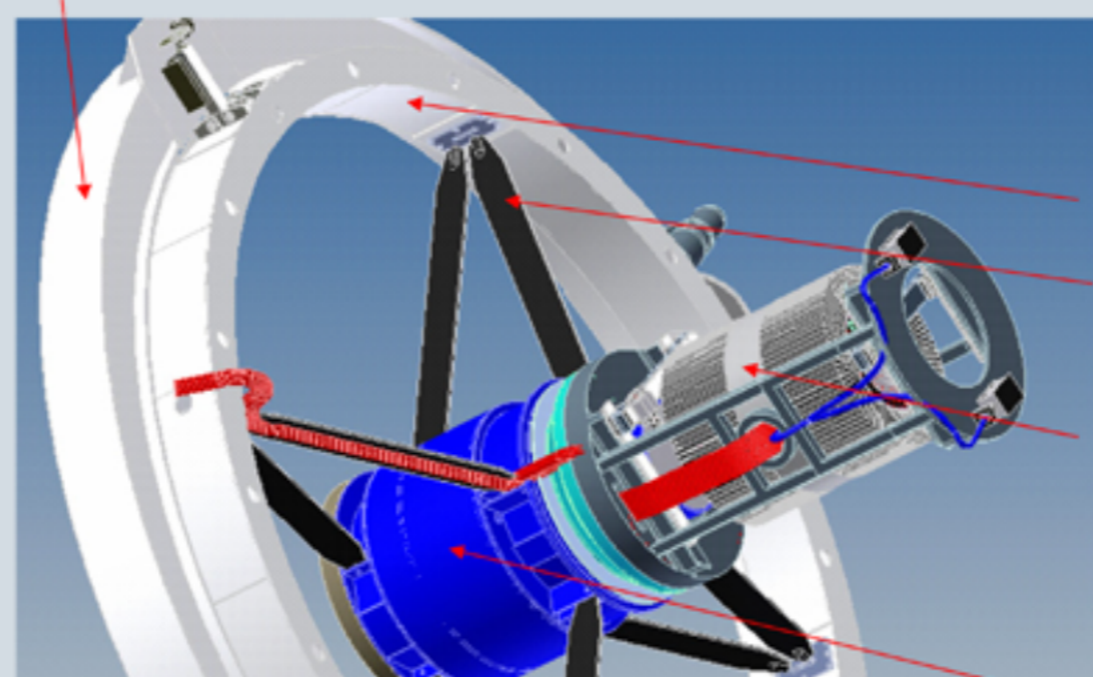
[Home](#) · [Overview](#) · [Science](#) · [Instrument](#) · [Team](#) · [Consortium](#) · [News](#) · [Papers](#) · [Other MOS Projects](#) · [Project extranet](#) · [ING](#)



WEAVE

TELESCOPE TOP END CONCEPT LAYOUT
Prime Focus Centre Section

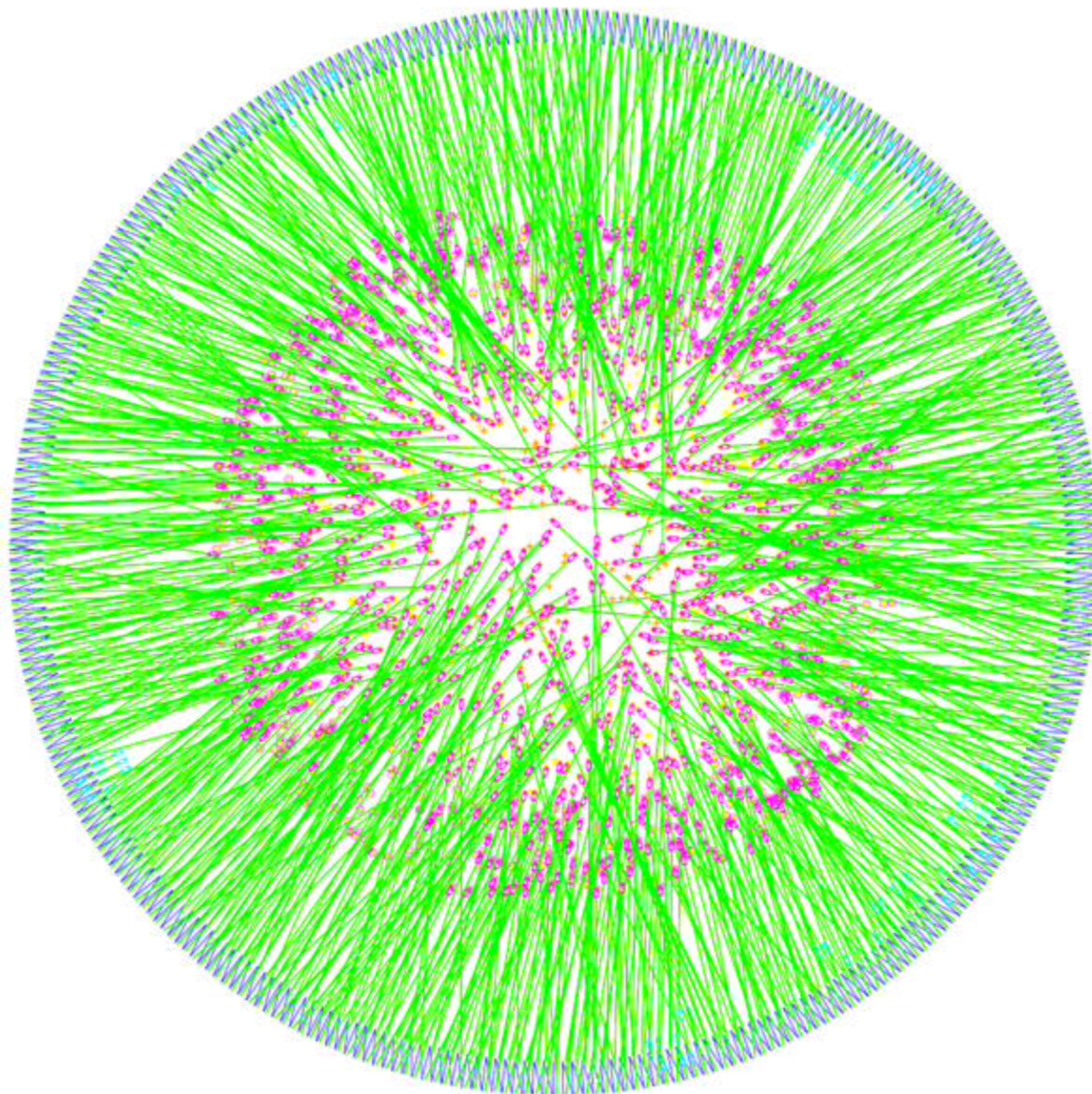
Telescope
Existing Top
Ring



- REQUIRED FOR WEAVE;
- New Flip Ring.
- New Vanes
- New Fibre Positioner
- New Centre Section Housing and Optics for Corrector and

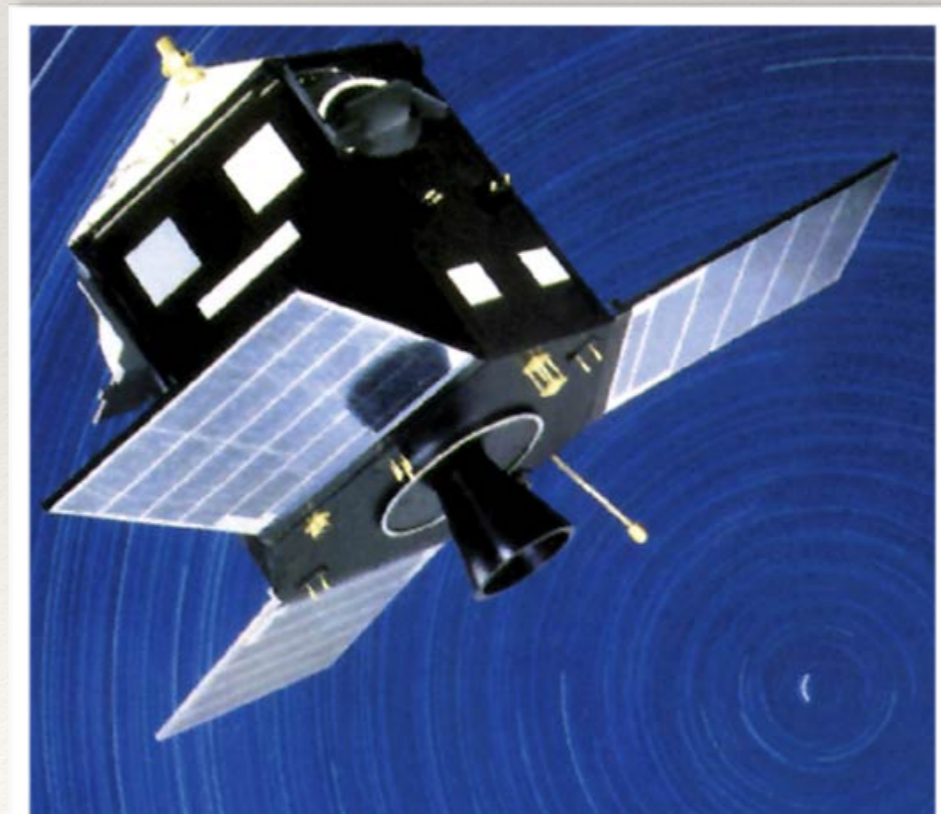
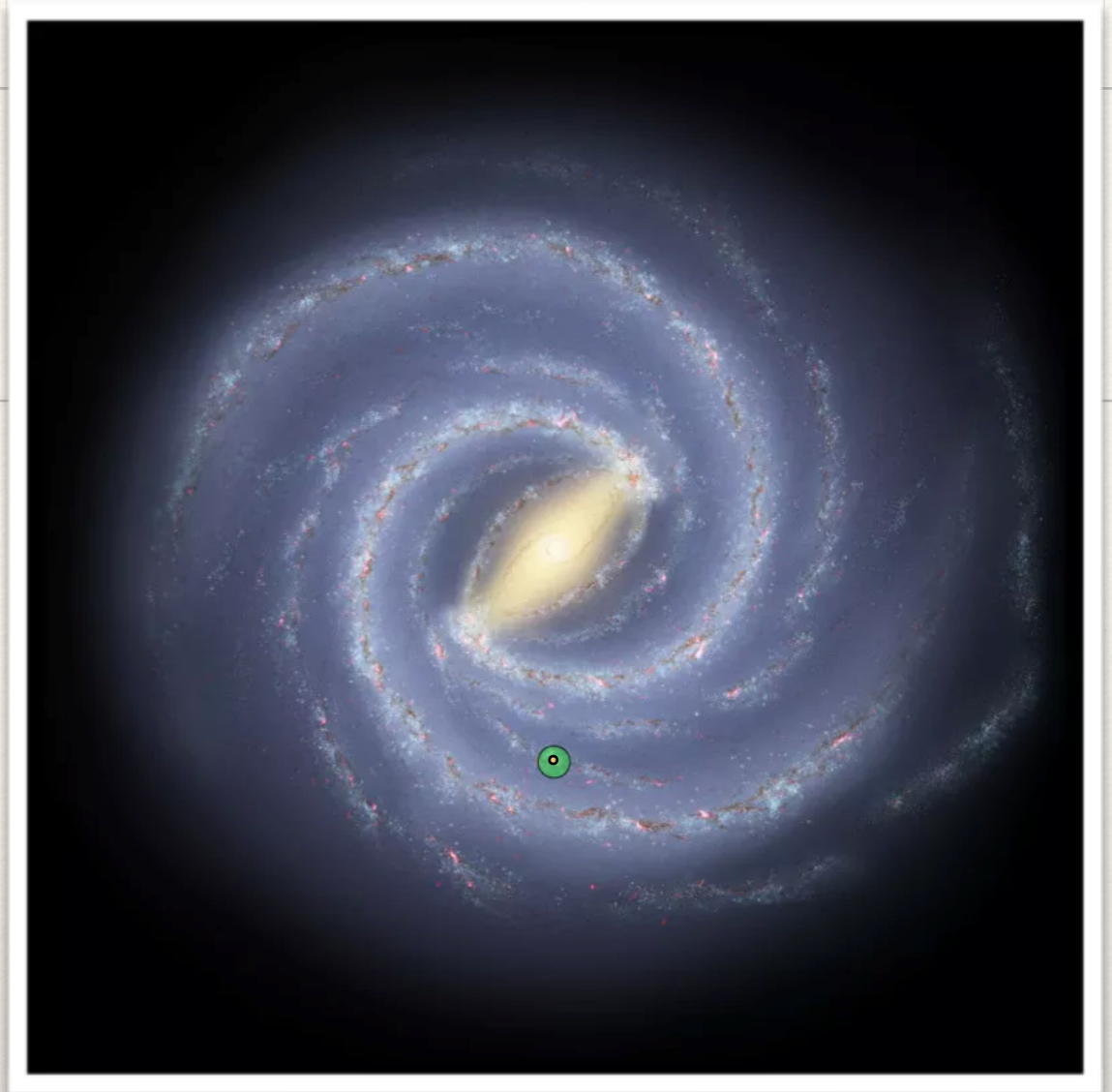


A computer simulation shows the complexity of weaving 920 fibres to acquire their targets. Each green line represents a single fibre and the purple dots represent the 920 fibre crossings. In this particular example there are 1962ApJ...136..748E



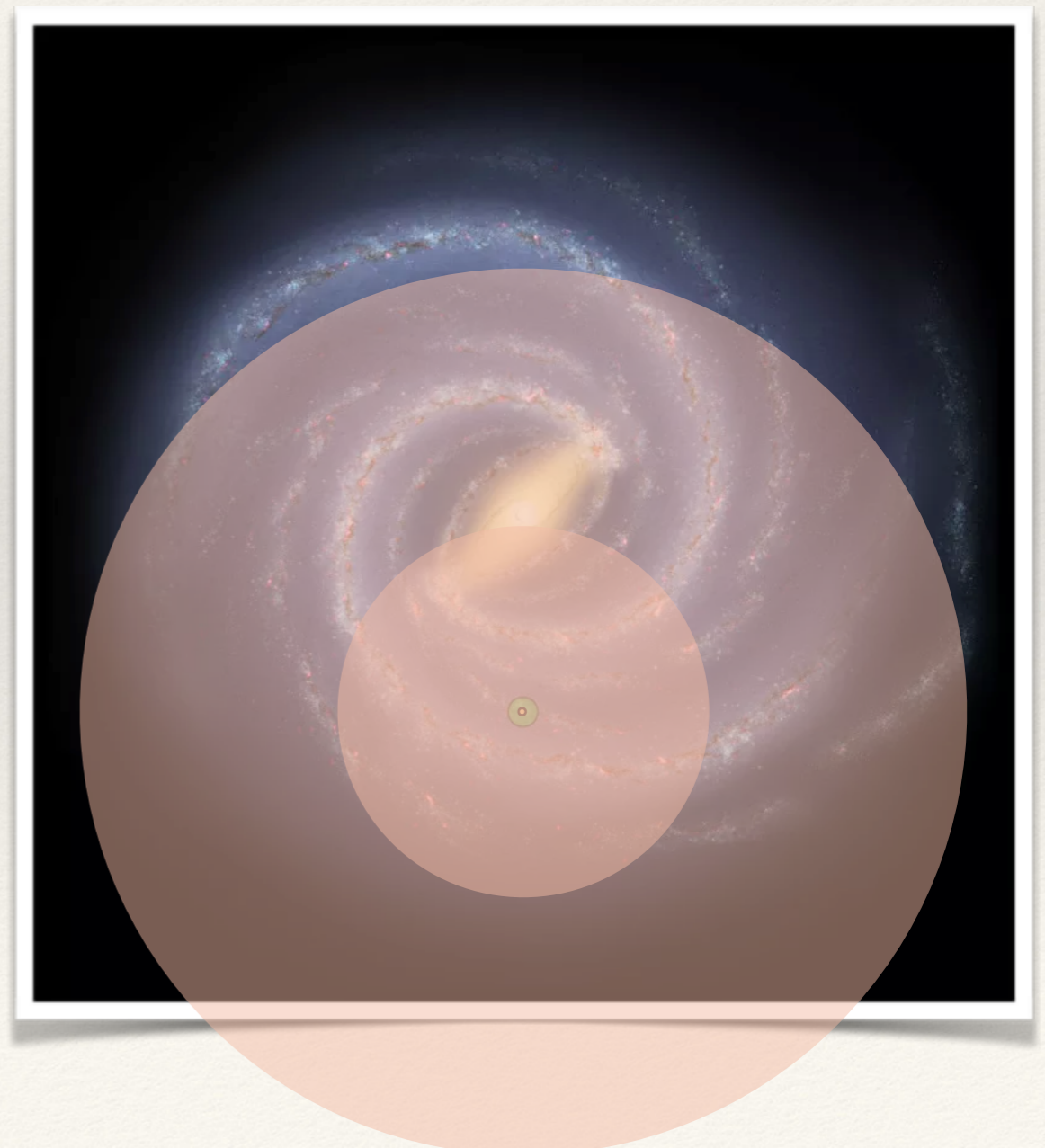
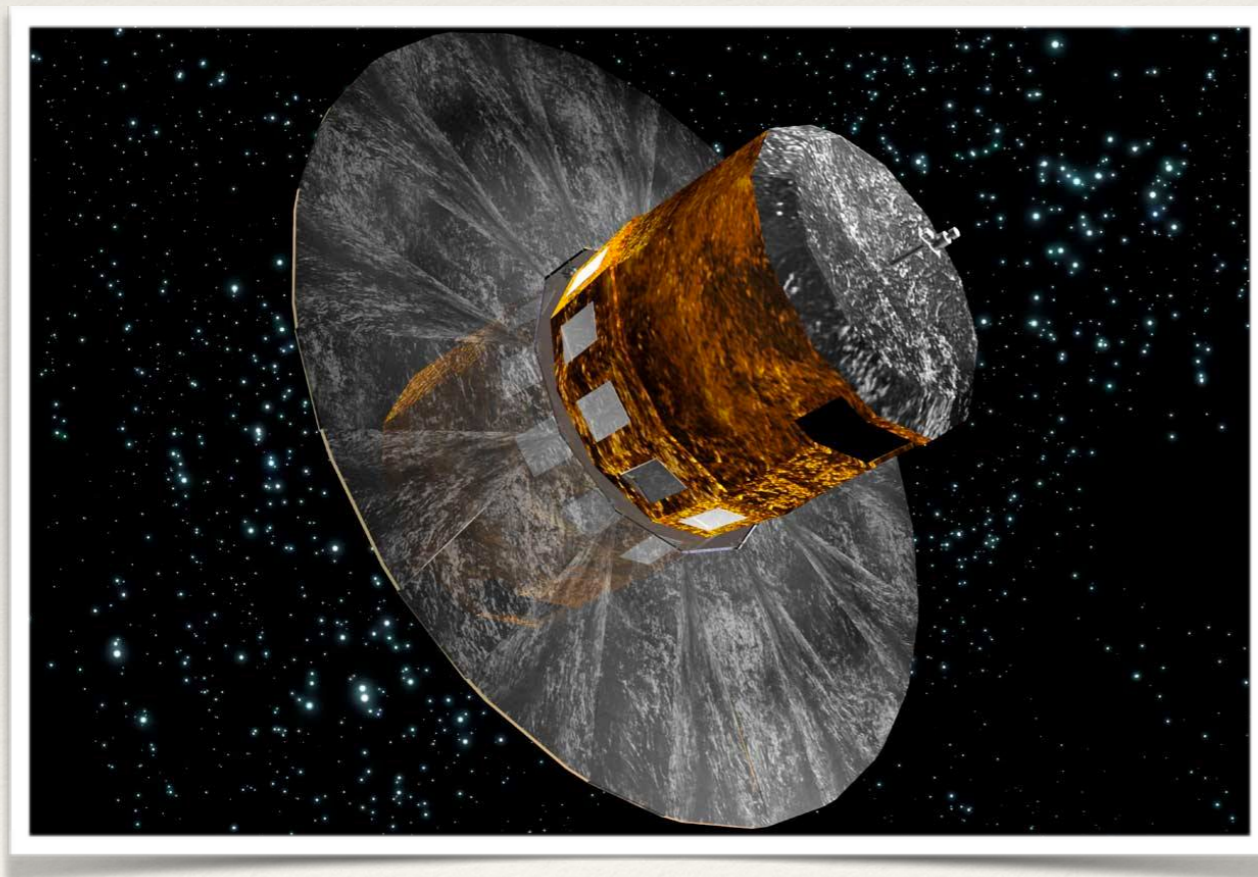
HIPPARCOS

- ❖ 1989-93
- ❖ Korlátozott képességek...
- ❖ 120 000 csillagra parallaxis
- ❖ milliívmásodperces pontosság
- ❖ 2 millió csillagra asztrometria



Gaia - emeljük a tétet

- ❖ Térképezzük fel a fél galaxist!



❖ HIPPARCOS

- ❖ parallaxis: 120 000
- ❖ asztrometria: 2 millió
- ❖ fotometria: 2 millió
- ❖ színindex: 0
- ❖ radiális sebességek: 0
- ❖ Naprendszer: 48

❖ Gaia elvárások

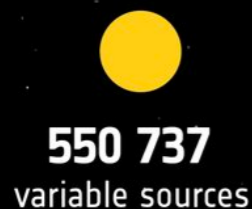
- ❖ parallaxis: 100 millió (10% hiba)
- ❖ asztrometria: > 1 milliárd
- ❖ fotometria: > 1 milliárd
- ❖ színindex: > 1 milliárd
- ❖ radiális sebességek: 150 millió
- ❖ Naprendszer: százezrek

Gaia Data Release 2: T-9 nap

Gaia Data Release 2: T-9 nap

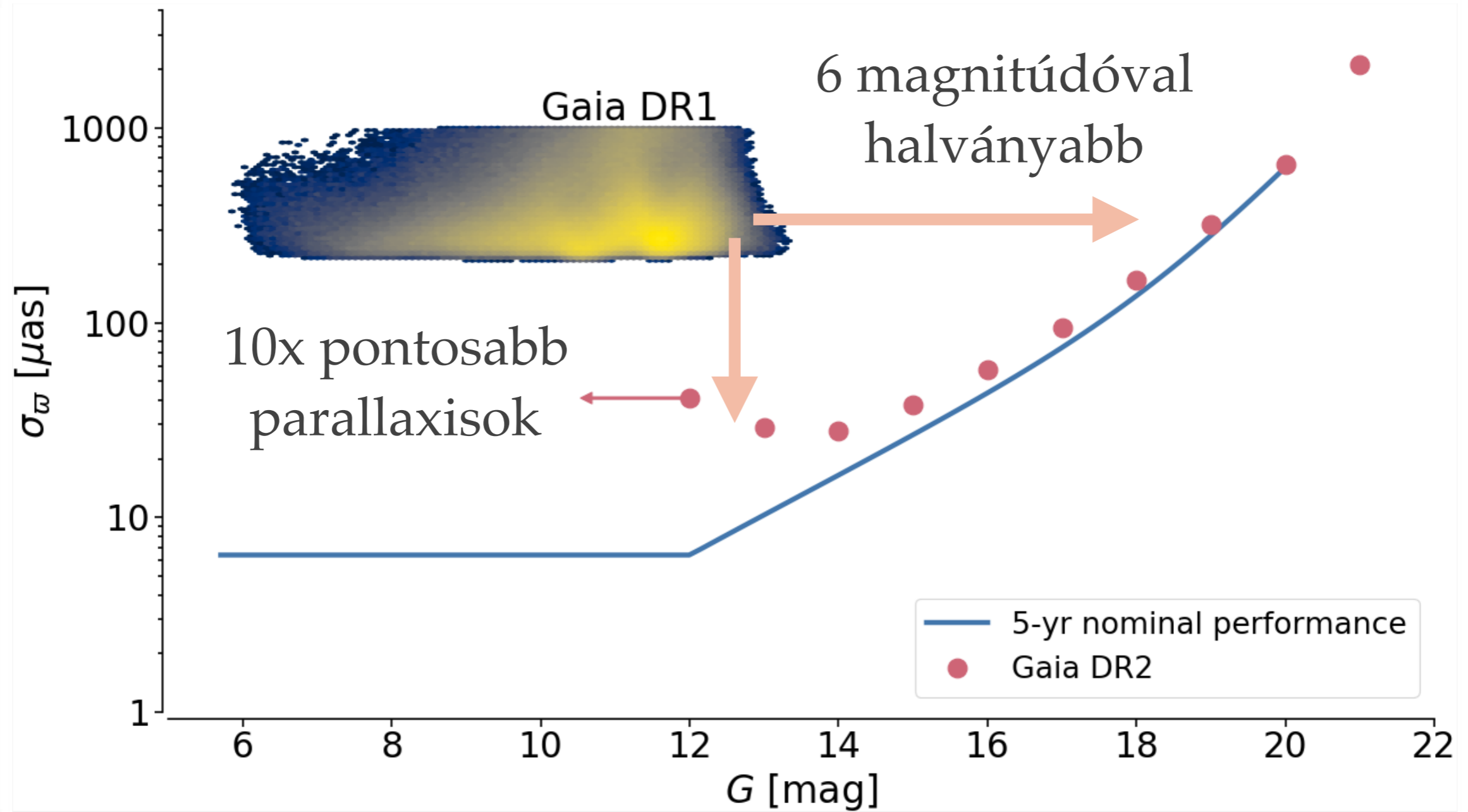


→ HOW MANY STARS WILL THERE BE IN THE SECOND GAIA DATA RELEASE?

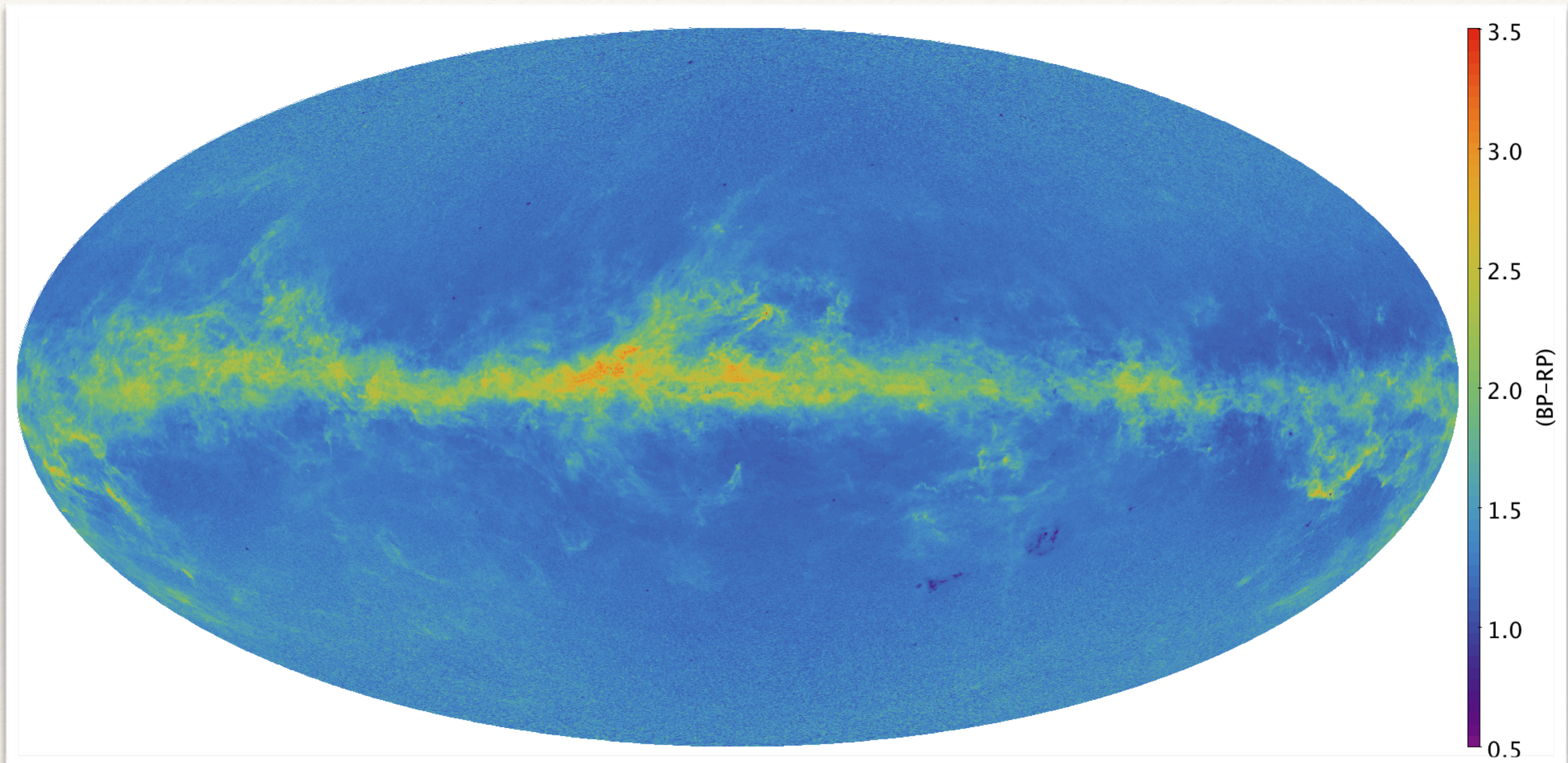


Április 25-én minden kiderül...?

“You are free to use these for previews of DR2 in your institute.”

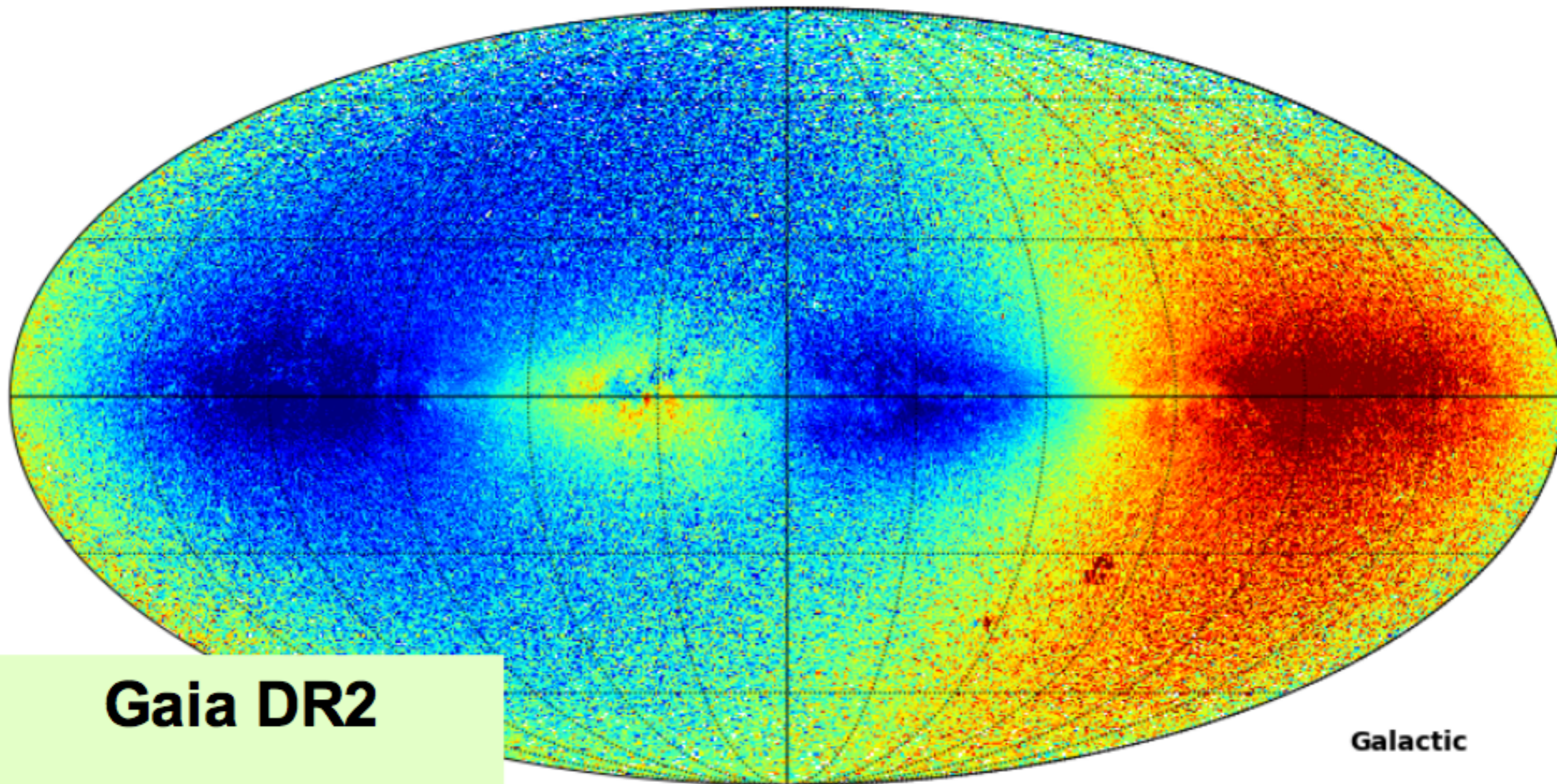


Az égbolt színe (BP-RP színindex)



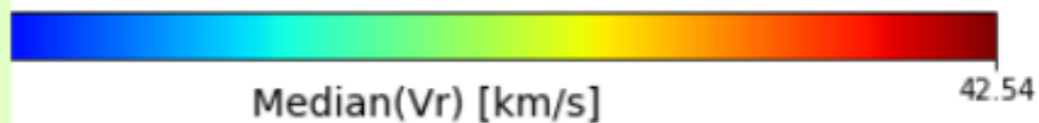
A Tejútrendszer sebessége

Mollweide view



Gaia DR2

25 April 2018

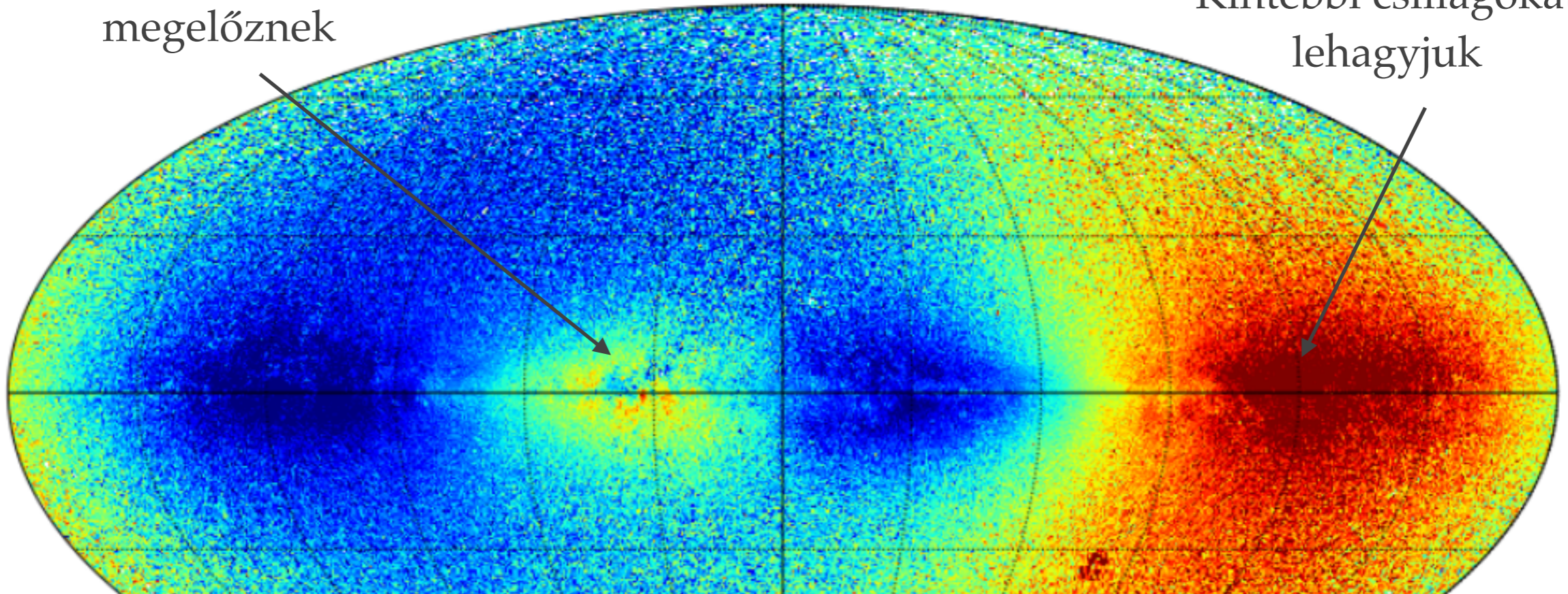


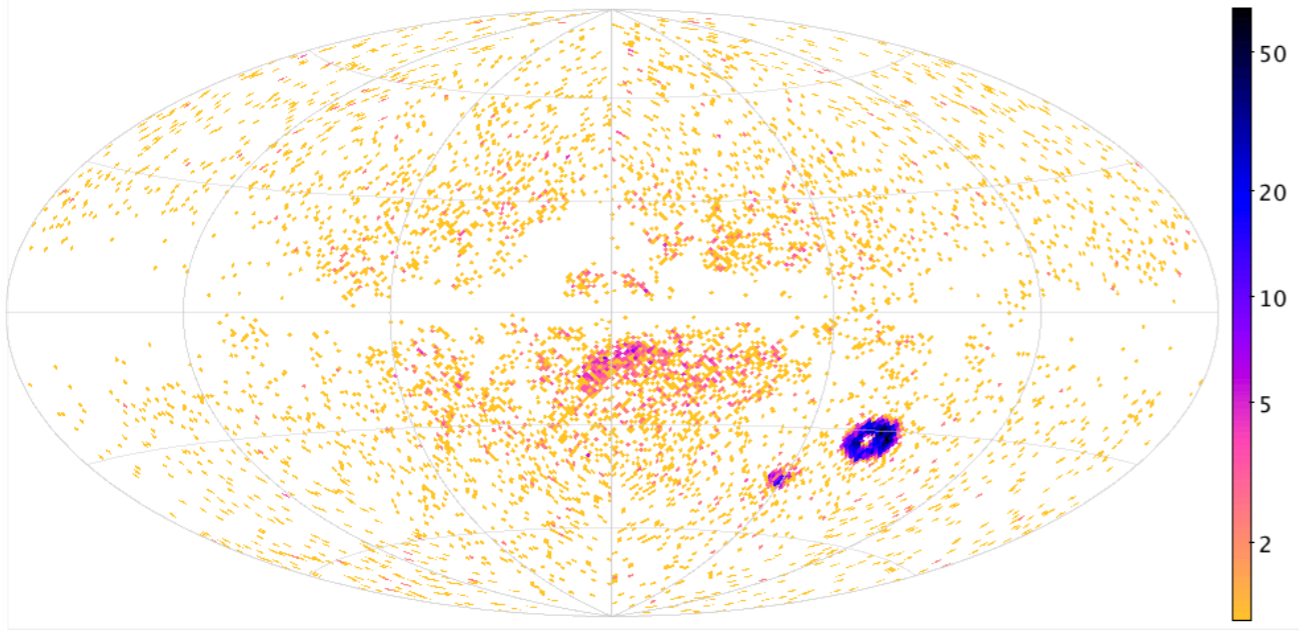
A Tejútrendszer sebessége

Bentebbi csillagok megelőznek

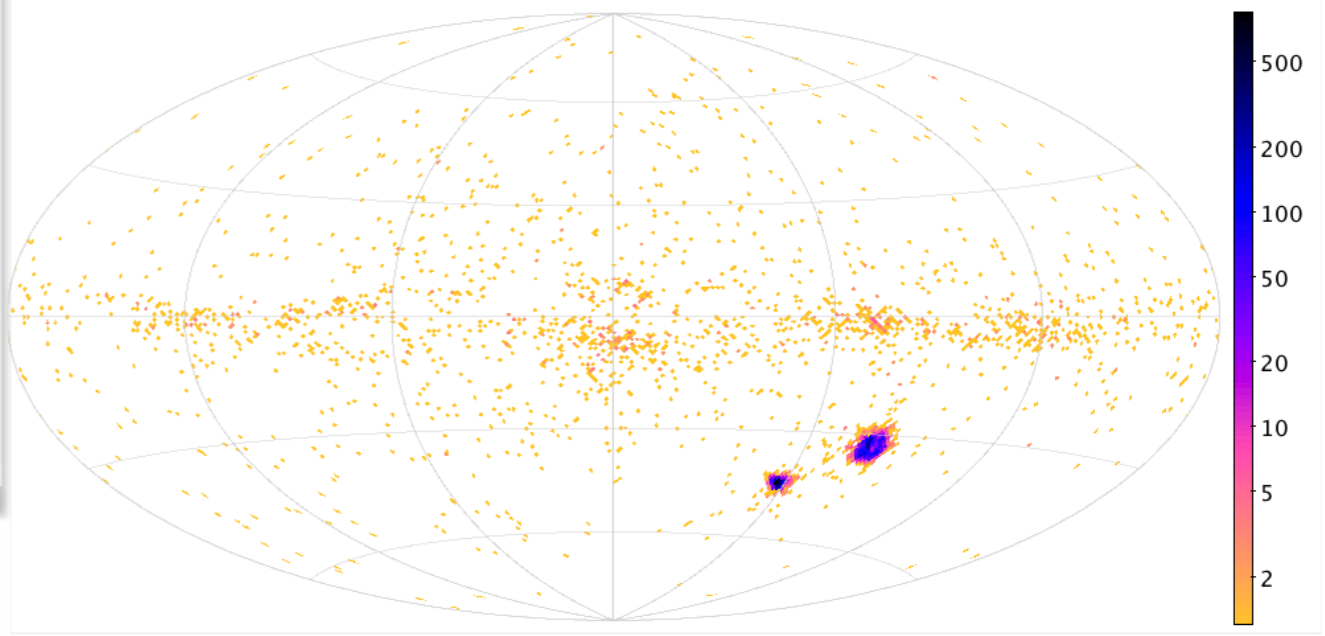
Mollweide view

Kintebbi csillagokat le hagyjuk

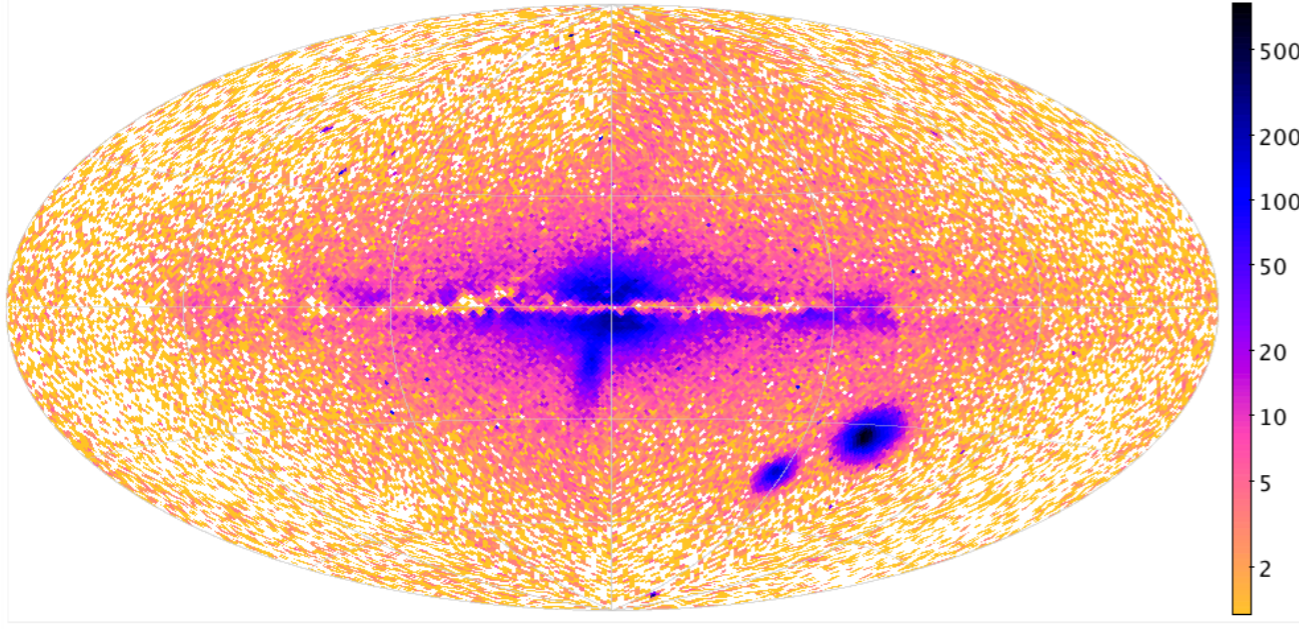




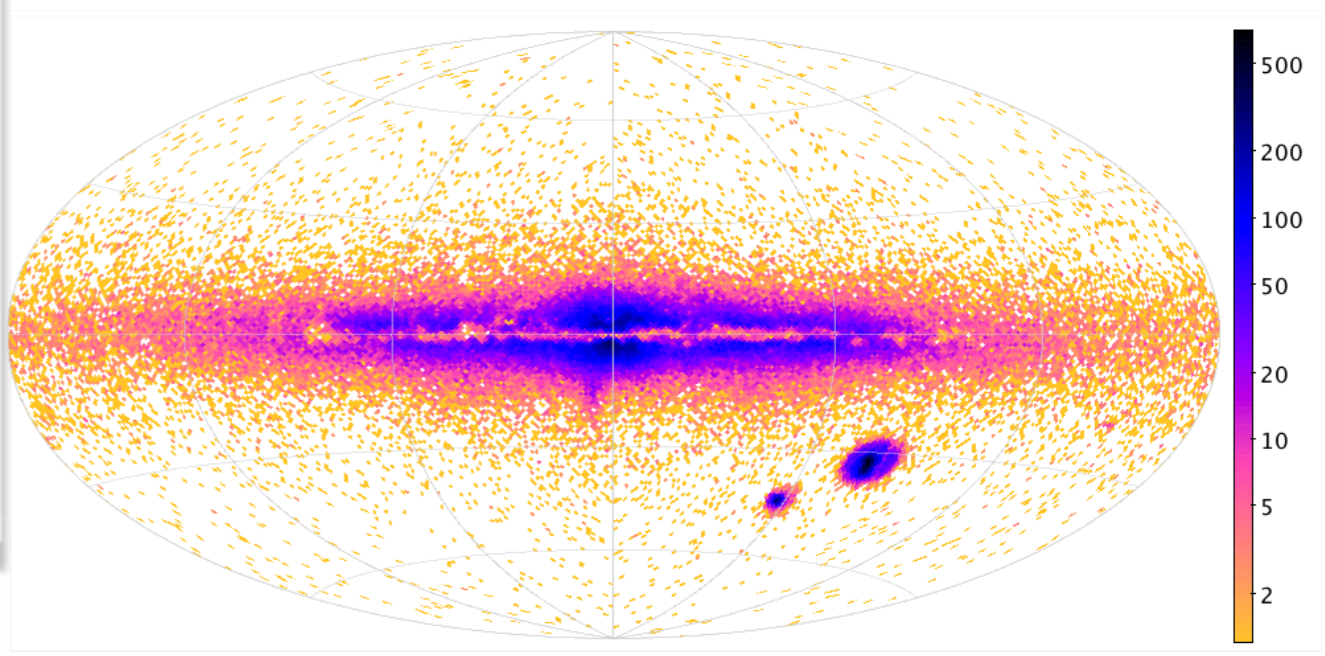
delta Scuti/SX Phoenicis



cefeidák



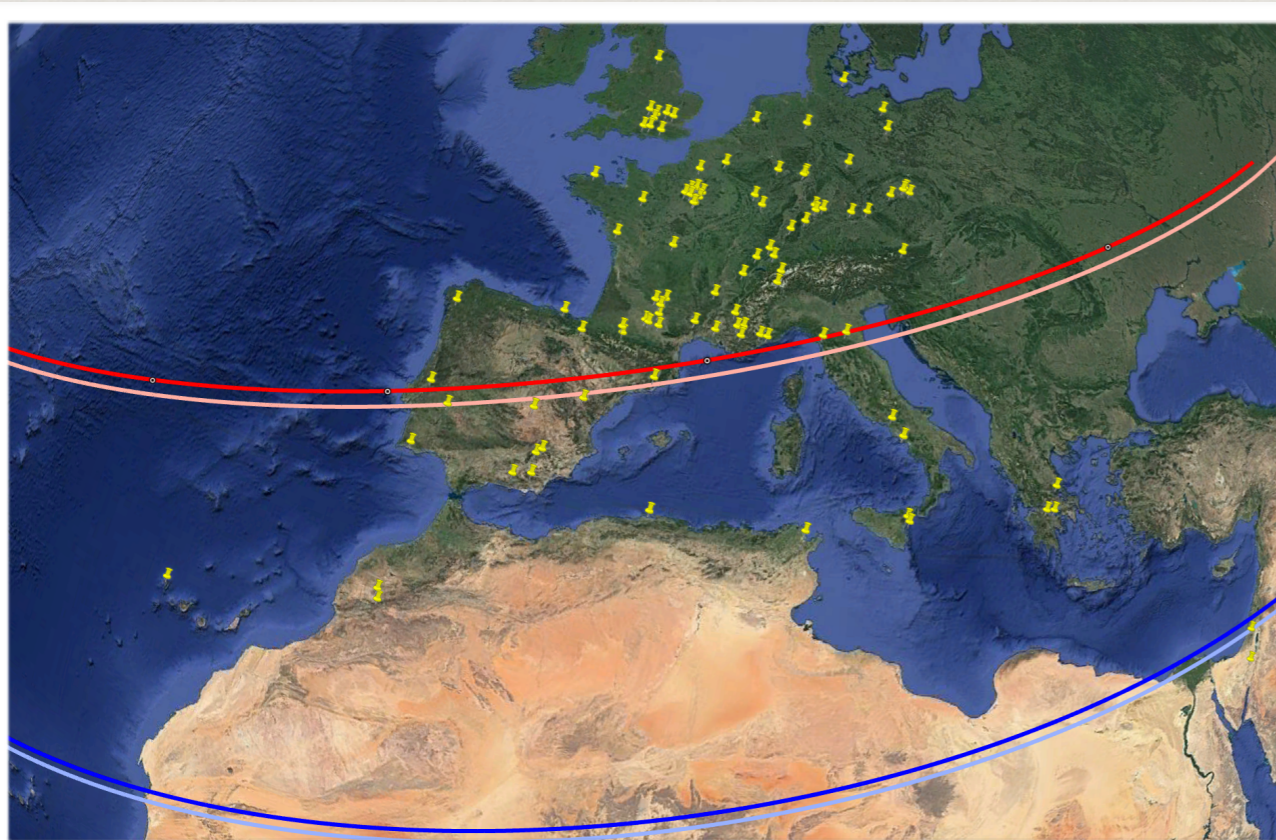
RR Lyrae



hosszúperiódusú változók

DR2 első eredménye

- ❖ Triton okkultáció, 2017. 10. 02. - légkör fénytörése felvillanást okoz a középpontban
- ❖ Triton kb. 100 km széles folt \rightarrow 5 milliívmásodperc széles
- ❖ 453 csillag előzetesen a DR2 adatokból



DR2 első eredménye

- ❖ Triton pályájának megváltozását okoz a közeli égitest
- ❖ Triton pályájának megváltozását okoz a közeli égitest
- ❖ 453 új égitest



- ❖ *A 2020-as évek csillagászata:*
 - ❖ *folytonos fotometria minden fényesebb csillagról*
 - ❖ *6D térkép a Tejútrendszer felénk eső feléről*
 - ❖ *fizikai paraméterek elképesztő gazdagsága*
- ❖ *...és végleges belefulladás a mindent elöntő adatokba.*